Dissertation

Stefan Linsler

Aus dem Bereich Physiologie
Theoretische Medizin
der Medizinischen Fakultät
der Universität des Saarlandes, Homburg/Saar

„Studies of the different neuronal presynaptic vesicle pools and the role of the presynaptic protein α-/β-SGT in neurons "

Dissertation zur Erlangung des Grades eines Doktors der Medizin
der Medizinischen Fakultät
der UNIVERSITÄT DES SAARLANDES
2006

Vorgelegt von: Stefan Linsler
Geb. am: 24.11.1980 in Saarlouis

1. Tag der Promotion: ....

2. Dekan: Prof. Montenarh

3. Berichterstatter: ....

Anschrift: Physiologisches Institut, Geb. 59;
          Universitätskliniken des Saarlandes; 66421 Homburg

Erklärung gemäß §7 Abs. 1 Nr.4

Ich erkläre hiermit an Eides Statt, dass ich die vorliegende Arbeit ohne unzulässige Hilfe Dritter und ohne Benutzung anderer als der angegebenen Hilfsmittel angefertigt habe. Die aus anderen Quellen direkt oder indirekt übernommenen Daten und Konzepte sind unter Angabe der Quelle gekennzeichnet.

Bei der Auswahl und Auswertung folgenden Materials haben mir die nachstehend aufgeführten Personen in der jeweils beschriebenen Weise unentgeltlich/entgeltlich geholfen:

1. ....
2. ....

Weitere Personen waren an der inhaltlich-materiellen Erstellung der vorliegenden Arbeit nicht beteiligt. Insbesondere habe ich nicht die entgeltliche Hilfe von Vermittlungs- bzw. Beratungsdiensten (Promotionsberater/innen oder anderer Personen) in Anspruch genommen. Außer den Angegebenen hat niemand von mir unmittelbar oder mittelbar geldwerte Leistungen für Arbeiten erhalten, die im Zusammenhang mit dem Inhalt der vorgelegten Dissertation stehen.

Die Arbeit wurde bisher weder im Inland noch im Ausland in gleicher oder ähnlicher Form in einem anderen Verfahren zur Erlangung des Doktorgrades einer anderen Prüfungsbehörde vorgelegt.

Ich versichere an Eides statt, dass ich nach bestem Wissen die Wahrheit gesagt und nichts verschwiegen habe.

Vor Aufnahme der vorstehenden Versicherungen an Eides statt, wurde ich über die Bedeutung einer eidesstattlichen Versicherung und die strafrechtlichen Folgen einer unrichtigen oder unvollständigen eidesstattlichen Versicherung belehrt.

....
Ort, Datum

....
Unterschrift des Promovierenden

....
Unterschrift der die Versicherung an Eides statt aufzunehmenden Beamten

List of contents

Abbreviations

A	Ampere
α-SNAP	α-soluble NSF attachment protein
ATP	adenosine triphosphate
BoNT/A-G	botulinum neurotoxins A-G
bp	base pair
BSA	bovine serum albumine
C	Coulomb
CNS	central nervous system
CSP	cysteine string protein
Da	Dalton
dH$_2$O	distilled water
DMEM	Dulbecco´s modified Eagle´s medium
DNA	desoxyribonucleic acid
dNTP	desoxyribonucleotide
EDTA	Ethylendiaminetetraacetate
EGTA	Ethylenbis-(oxyethylennitrilo-)tetraacetic acid
EPSC	excitatory postsynaptic currents
FCS	fetal calf serum
GFP	green fluorescent protein
HBBS	Hank´s balanced salt solution
HEPES	4-(2-Hydroxyethyl)-1-piperazine ethansulfonic acid
HSC70	heat shock cognate protein of 70 kDa
Hz	Hertz
I	current
IPSC	inhibitory postsynaptic currents
LDCV	large dense core vesicles
NP-EGTA	nitrophenyl-EGTA
NSF	N-ethylmaleimide sensitive factor
P	postnatal day

PBS	phosphate buffered saline
PCR	polymerase chain reaction
PKA	protein kinase A
PKC	protein kinase C
RIM	Rab3-interacting molecule
RRP	readily releasable pool
RT	room temperature
SDS	sodiumdodecyl sulfate
SEM	standard error of the mean
SFV	Semliki Forest virus
SGT	small glutamine-rich tetratricopeptide repeats containing protein
SNAP-25	synaptosome associated protein of 25 kDa
SNARE	soluble NSF attachment protein receptors
SRP	slowly releasable pool
SV	synaptic vesicles
TAE-buffer	Tris acetate EDTA buffer
TeNT	tetanus neurotoxin
UPP	unprimed pool
UV	ultra violet
VAMP	vesicle associated membrane protein
v/v	volume per volume
w/v	weight per volume

1.1 Summary

The formation and stability of the ternary SNARE complex consisting of synaptobrevin, syntaxin and SNAP-25 (synaptosome-associated protein of relative molecular mass of 25 kDa) play a central role in the molecular mechanism of neurotransmitter release. In order to investigate the physiological role of SNAP-25 on release rates and size of vesicle pools in neurons, I overexpressed SNAP-25Δ9 in cultured mouse hippocampal neurons. The overexpressed protein SNAP-25Δ9 corresponds to the Botulinum neurotoxin A cleavage product and leads to a selective reduction of the RRP (readily releasable pool) in chromaffin cells.

I examined neurotransmitter release following action potentials induced by depolarisation, and following applications of hypertonic extracellular sucrose mixtures. Action potential induced release of neurotransmitter is Ca^{2+} dependent while release induced by hypertonic solutions has been shown to be independent of Ca^{2+} entry. I measured transmitter release using electrophysiological methods, comparing the amounts of release and the rates of release following electrical stimulation and hypertonic sucrose application. With the appropriate experimental protocol I could determine whether the same vesicle pools are released with these two types of stimuli.

My results show that one can measure two time constants and different kinetics of neurotransmitter release in hippocampal neurons during high frequency stimulations, consistent with earlier reports. These two time constants demonstrate, that a SRP (slowly releasable pool) and a RRP of vesicles exist in neurons comparable to the two reported vesicle pools, SRP and RRP, in chromaffin cells. The charge transfer of neurons over the cell membrane in case of the SNAP-25Δ9 - mutant is not reduced in case of hypertonic sucrose solution treatment in comparison to control cells and recovery of the EPSC amplitude after sucrose application takes longer and the degree of recovery is lower than that observed after high frequency stimulation. So I derive from my results the hypothesis that sucrose solution released vesicles not only from the RRP but also from the SRP and the UPP (unprimed pool) in neurons. The hypertonic solution induced release

is thought to engage the exocytotic machinery at some step after docking and the most likely releasing mechanism is a mechanical one, like a stress induced change on tension.

The SGT (small glutamine-rich tetratricopeptide repeat-containing) protein is a cochaperone of Hsc70 (heat shock cognate protein of 70 kDa) and of CSP (cysteine string protein). There are two isoforms of the SGT protein: α-SGT, which is expressed ubiquitously, and β-SGT, which is exclusively expressed in the brain. SGT, Hsc70 and CSP combine to form a trimeric chaperone complex that is located on the synaptic vesicle surface and is important for the maintenance of a normal synaptic function, since it is required for delivery of synaptic vesicles to the presynaptic terminal. In order to investigate the physiological role of SGT in the brain, α-/β-SGT lacking mice were generated and their synaptic function was examined using electrophysiological measurements to analyse the EPSC amplitude, vesicle pool size and rate of synaptic depression.

α-/β-SGT lacking mice exhibit a lower body size and weight but no obvious effects on synaptic transmitter release in cell culture at postnatal days 8 - 14. At postnatal days 21 - 24 the SGT double knockout mice exhibit no severe phenotypic changes in neuronal cell culture with the exception of a slight reduction of the slow time constant of depression in double knockout neurons. This results differ from those from CSPα lacking mice, which develop severe neurological disorders and electrophysiological dysfunction after the third postnatal week. I was unable to maintain α-/β-SGT knockout neurons in cell culture for more than 3 – 4 weeks and therefore I was unable to exclude an effect in SGT double knockout mice older than 4 weeks.

As mentioned above SGT is part of the synaptic trimeric complex CSP/SGT/Hsc70 in neurons, which seems to play an important role in neurotransmission as reported in recent studies. However my results demonstrate that SGT is not an essential player in the complex as the loss of SGT does not prevent the development of normal synaptic function. This result challenges the functional role of SGT as an important cochaperone in neurons. It is possible that Hsc70 is able to adapt to the

loss of SGT protein as cochaperone and to abide the function of the trimeric chaperone complex in neurons in case of α-/β-SGT lacking mice.

1.2 Zusammenfassung

Die Bildung und Stabilität des dreifachen SNARE-Komplexes, bestehend aus den Proteinen Synaptobrevin, Syntaxin und SNAP-25 (Synaptosom-assoziiertes Protein der relativen Molekülmasse von 25 kDa), spielen eine zentrale Rolle im molekularen Mechanismus der Neurotransmitterfreisetzung. Mit dem Ziel die physiologische Rolle von SNAP-25 in Bezug auf Freisetzungskinetik und Größe der Vesikelpools in Neuronen zu untersuchen, überexprimierte ich SNAP-25Δ9 in hippocampalen Neuronen von Mäusen. Die Überexpression des Proteins SNAP-25Δ9 entspricht dem Spaltungsprodukt des SNAP-25 Proteins nach Behandlung mit Botulinum Toxin A und führt in Chromaffinzellen zu einer selektiven Reduktion des RRP (readily releasable pool = schnell freisetzbarer Vesikelpool).

Ich untersuchte die synaptische Neurotransmitterfreisetzung, indem ich zum einen die synaptische Antwort nach Depolarisation der Neurone maß und zum anderen die Neurotransmitterfreisetzung nach Verabreichung von hochosmolarer Saccharoselösung auf das gesamte Neuron. Die Aktionspotential induzierte Neurotransmitterfreisetzung ist Ca^{2+}-abhängig, wohingegen die Neurotransmitter-freisetzung, die durch Verabreichung von hochosmolaren Lösungen verursacht ist, Ca^{2+}-unabhängig ist. Ich verglich die Summe der Neurotransmitterfreisetzung und die Freisetzungskinetik nach elektrischen und nach hochosmolaren Stimuli. Mit meinem experimentellen Protokoll konnte ich ermitteln, ob die gleichen Vesikelpools der Präsynapse durch diese beiden unterschiedlichen Stimulationsarten freigesetzt werden.

Meine Ergebnisse zeigen für Neurone deutlich, dass man zwei Zeitkonstanten und zwei unterschiedliche Kinetiken der Neurotransmitterfreisetzung während hochfrequenter elektrischer Stimuli bestimmen kann. Es liegt nahe zu folgern, dass diese zwei Zeitkonstanten der Freisetzung des SRP (slowly releasable pool = langsam freisetzbarer Vesikelpool) und des RRP in Neuronen entsprechen. Diese sind vergleichbar mit den zwei bereits nachgewiesenen Vesikelpools SRP und RRP in Chromaffinzellen. Die freigesetzte Ladung an der neuronalen Zellmembran ist im Falle der SNAP-25Δ9-Mutanten nach Behandlung mit hochosmolarer

Saccharoselösung nicht nachweisbar verringert und das Wiederauffüllen der Vesikelpools nach Verabreichung von Saccharose verläuft langsamer und erreicht ein geringeres Endniveau als nach hochfrequenten Stimuli. So dass ich aus meinen Ergebnissen die Schlussfolgerung ziehe, dass die Verabreichung von hochosmolarer Saccharoselösung auf Neurone nicht nur den RRP freisetzt sondern auch den SRP und UPP (unprimed pool = „ungeprimter" Vesikelpool). Meine Hypothese ist damit im Widerspruch zu den bisherigen Studien, die aussagen, dass durch Verabreichung von hochosmolarer Lösung nur der RRP freigesetzt werden würde. Der Stress-induzierende Mechanismus der Neurotransmitterfreisetzung während der Saccharose-Verabreichung, der am ehesten durch den osmotischen Druck auf die Zellmembran entsteht, greift in die Freisetzungsmaschinerie der Vesikel nach dem Schritt des „Docking" der Vesikel ein.

SGT (engl. : kleines Glutamin – reiches Tetratricopeptid Repeat - enthaltendes) Protein ist ein Cochaperon von Hsc70 (engl. : Hitzeschock Protein mit der relativen Molekülmasse von 70 kDa) und von CSP (engl. : Cystein Ketten Protein). Es gibt zwei Isoformen des SGT Protein: α-SGT, das im ganzen Körper exprimiert ist, und β-SGT, das nur im Gehirn vorkommt. SGT, Hsc70 und CSP verbinden sich und bilden einen dreiteiligen Chaperon-Komplex, der an der Oberfläche der synaptischen Vesikel lokalisiert ist und wichtig für die Aufrechterhaltung der normalen synaptischen Funktion ist. Um die physiologische Rolle von SGT im Gehirn zu untersuchen, wurden α-/β-SGT Knockout-Mäuse generiert und deren synaptische Eigenschaften mit elektrophysiologischen Methoden untersucht. Dadurch konnte ich die EPSC Amplitude, die Größe der Vesikelpools und die Kinetik der synaptischen Depression bestimmen.

α-/β-SGT Knockout-Mäuse wiesen in den postnatalen Tagen 8 - 14 ein geringeres Körpergewicht und eine geringere Größe im Vergleich zu Wildtyp-Mäusen auf, aber in Zellkultur waren keine offensichtlichen Veränderungen der synaptischen Transmitterfreisetzung feststellbar. Auch später, in den postnatalen Tagen 21 - 24, zeigten die α-/β-SGT Knockout-Mäuse keine gravierenden Veränderungen des Phänotyps und in kultivierten Neuronen keine Änderungen der synaptischen

Funktion mit Ausnahme der langsamen Zeitkonstanten der Depressionskurve, die in Doppelknockout Mäusen geringfügig reduziert war. Diese Ergebnisse unterscheiden sich erheblich von denen in CSPα Knockout Mäusen, welche 21 Tage nach Geburt schwere neurologische Symptome und elektrophysiologische Funktionsstörungen entwickeln. Es gelang mir nicht die Neurone länger als 21 - 24 postnatale Tage in Kultur zu halten und elektrophysiologisch zu messen, so dass eine synaptische Veränderung oder Degeneration in α-/β-SGT Knockout-Mäusen, die älter als 4 Wochen sind, nicht auszuschließen ist.

Wie oben erwähnt ist SGT Bestandteil des synaptischen dreiteiligen Komplexes CSP/SGT/Hsc70 in Neuronen. Meine Ergebnisse zeigen, dass der Verlust von α- und β-SGT keine schweren funktionalen Defizite verursacht und die Entwicklung und Aufrechterhaltung der normalen synaptischen Funktion nicht beeinträchtigt ist. Das heißt, dass die Funktion des dreiteiligen Komplexes als Chaperon an den präsynaptischen Vesikeln ohne SGT aufrechterhalten werden kann. Die Funktion von SGT als wichtiges Cochaperon in Neuronen ist daher fragwürdig. Eine Möglichkeit ist, dass Hsc70 fähig wäre, den Verlust des SGT als Cochaperon auszugleichen und dadurch die Funktion des dreiteiligen Chaperon - Komplexes in α-/β-SGT Knockout-Mäusen aufrechtzuerhalten.

2. Introduction

2.1 Synapses

The human brain contains 10^{12} neurons. Each forming thousands connections with other neurons. These connections are called synapses. The term 'synapse' was first used by Foster and Sherrington in 1897. There are about 10^{15} synapses in the human brain. Synapses are structures of high interest for neuroscience because they are the sites of contact between neurons, of learning and memory, and the target of many drugs and toxins. Many neurological diseases are caused by a degeneration or functional disorder of synapses.
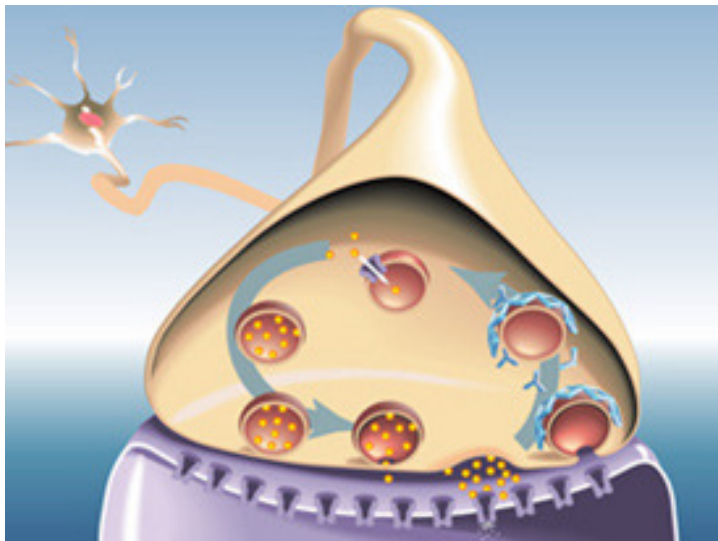
Figure 2.1: stylized model of a neuronal synapse: Synaptic vesicles (brown) move through the vesicle cycle (blue arrows). The cycle begins with vesicle filling (top center) and proceeds through the steps of docking and priming. Primed vesicles release their contents (yellow) and are then recycled via endocytosis. (reproduced from http:// www.neuroscience.med. utah.edu/Faculty/ Jorgensen.html

The information in neurons is proceeded using a combination of electrical and chemical signals. Along a neuronal membrane information is transmitted by an electrical signal caused by ionic flow through ion channels in the membrane: this phenomenon is called the action potential (Hodgkin and Huxley, 1952). The communication between two neurons usually occurs via a chemical signal at a

synapse. In mammalians, synaptic transmission is mediated by a variety of neurotransmitters. Neuronal synapses are composed of two compartments: the presynaptic terminal in the axon and the postsynaptic membrane of the target cell, which are separated by a very small synaptic cleft. At such synapses an action potential, generated at the axon hillock of a presynaptic neuron, travels along the axon to the presynapse where it causes the opening of voltage-gated Ca^{2+} channels. Ca^{2+} ions entering the nerve terminal trigger the rapid release of vesicles containing neurotransmitter into the synaptic cleft. The binding of the released neurotransmitter to receptors on the postsynaptic neuron leads to either opening of ligand-gated ion channels causing an electrical signal - called synaptic potential -, or biochemical events: For example release of intracellular calcium or phosphorylation of proteins. These changes modify the activity of the postsynaptic neuron. The synaptic potential then eventually triggers in summation with other synaptic potentials a response which can generate an action potential in the following axon (Hall, 1992; Sargent, 1992).

2.2 Presynapse and synaptic vesicles

The presynaptic compartment, also called presynaptic element or presynapse, is usually an axon terminal. The terminal typically contains small membrane-enclosed spheres, about 50 nm in diameter, called synaptic vesicles. These vesicles store neurotransmitter. Many axon terminals also contain larger vesicles, about 100 nm in diameter, called secretory granules or large dense-core vesicles (LDCVs), because they contain soluble proteins that appear dark in the electron microscope.

The release of neurotransmitter from the presynaptic terminal is caused by exocytotic fusion of synaptic vesicles at the active zone – a specialized area of the presynaptic plasma membrane. The active zone is aligned with the synaptic cleft and the postsynaptic density to form a synaptic signalling complex (Fernandez-Chacon and Sudhof, 1999). The amount of neurotransmitter released at the synapse determines how strongly the postsynaptic neuron is excited. This depends on the number of synaptic vesicles in the primed state and on the release probability of

single vesicles, which is normally smaller than 0.05 for each presynaptic vesicle. Release probability of synaptic vesicles is very heterogeneous in among types of synapses.

Studies of giant synapses in the squid nervous system showed that exocytosis occurs very rapidly – within 0.2 msec of the Ca^{2+} influx into the axon terminal. Exocytosis is rapid because Ca^{2+} enters at the active zone, precisely where synaptic vesicles are ready and waiting to release their contents (Sugimori et al., 1994). In this local "microdomain" around the active zone, Ca^{2+} can achieve very high concentrations.

Synaptic vesicles are small organelles of variable size and their membrane contain about 20-40 distinct types of proteins and approximately 20,000 phospholipid molecules (Huang and Mason, 1978; Jahn and Sudhof, 1994) in a ratio of about 2:1 with cholesterol (Nagy et al., 1976).

The synaptic vesicles, which play a key role for neurotransmitter release, must undergo several modifications in the so-called synaptic vesicle cycle. A large number of presynaptic proteins are involved in this cycle with specific roles to play in the various steps of the cycle (Sudhof, 1995; Fernandez-Chacon and Sudhof, 1999).
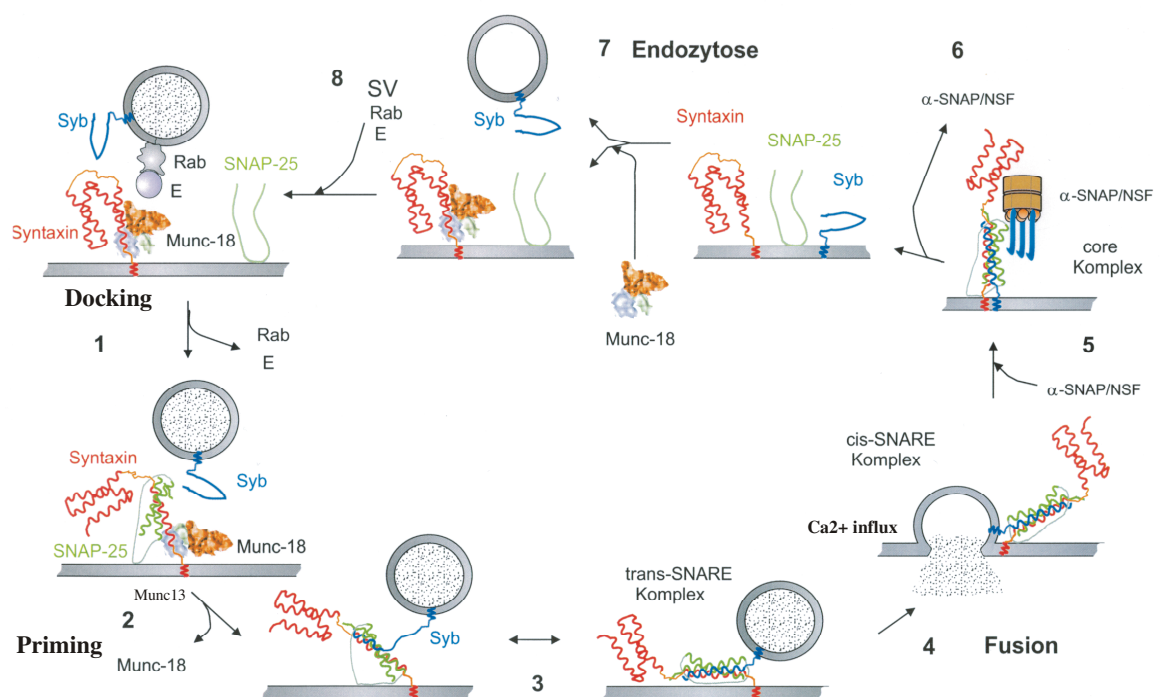
Figure 2.2: Different steps of the synaptic vesicle cycle including some of the important proteins (modified from unpublished figure from Ulf Matti and Thomas Binz):

Synaptic vesicles translocate to the active zone of the plasma membrane where they are anchored through a process called docking, in which the presynaptic protein Munc18-1 is involved (step 1). Docked vesicles are then rendered fusion-competent by a process called priming - mediated by Munc13´s (step2 and 3). Increase of intracellular Ca^{2+} through opening of voltage-gated calcium channels leads to fusion of synaptic vesicles with the plasma membrane and to the release of neurotransmitter into the synaptic cleft (step4). The fusion is mediated by the SNARE complex proteins SNAP25, syntaxin and synaptobrevin which build the so-called ´fusion pore`. The vesicle is then retrieved through clathrin-mediated endocytosis (step 5, 6 and 7). They fuse with endosomal compartments in the presynapse or can alternatively be directly refilled with neurotransmitter without passing through endosomes. The steps in the vesicle cycle are further described in the text. Step 2 and 3 can be assayed using the micro-island culture and patch clamping.

The membrane of synaptic vesicles and the presynaptic plasma membrane at the active zone must undergo an initial interaction that allows the maturation of the vesicles before release of neurotransmitter can be initiated. The first step is called docking. In recent studies, it has been demonstrated, that Munc18-1, a presynaptic protein, is involved in the docking of LDCVs and plays a role in the further development of synaptic vesicles (Voets et al., 2001; Korteweg et al., 2005; Weimer and Richmond, 2005). It is still unclear how Munc-18 mediates docking. Another protein complex, that appears to be involved is the Rab3-RIM complex (Johannes et al., 1998; Schluter et al., 2002; Schluter et al., 2004; Schluter et al., 2006).

Not all docked vesicles can release their neurotransmitter content immediately. Synaptic vesicles must undergo a second process, called priming, that makes them competent for rapid Ca^{2+}-triggered membrane fusion. Those docked vesicles that are released immediately are considered to be ´primed´. Priming is believed to occur when the vesicular protein synaptotagmin interacts with the presynaptic membrane proteins SNAP-25 and syntaxin to build so called SNARE complexes (Rettig and Neher, 2002). The priming process is ATP – dependent and modulated by PKA (Nagy et al., 2004) and PKC (Gillis et al., 1996; Smith et al., 1998). The Munc13´s are important priming factors during this process (Aravamudan et al., 1999; Augustin et al., 1999; Richmond et al., 1999; Brose et al., 2000; Stevens et al., 2005) and interact with the SNARE proteins.

The primed vesicles undergo rapid exocytosis following an increase of the intracellular Ca^{2+} concentration. Intracellular Ca^{2+} rises in response to an action

potential cause of the opening of calcium channels after depolarisation in the presynaptic membrane, localized at the active zone.

The membrane of the synaptic vesicle and the membrane of the synaptic terminal at the active zone undergo fusion mediated by the SNARE complex proteins and build the so-called ´fusion pore`. Through that fusion pore the neurotransmitters are released. The molecular structure and mechanism of the fusion pore is unknown. It appears that lipids of the vesicles diffuse in to the plasma membrane while the proteins do not (Taraska et al., 2003; Fulop et al., 2005). The diameter of a fusion pore was estimated close to 1 nm (Richards et al., 2005). SNARE proteins likely stabilize the fusion pore. Recent studies have all indicated that the SNARE proteins are intimately involved in the last steps of exocytosis (Capogna et al., 1997; Xu et al., 1998; Xu et al., 1999b; Borisovska et al., 2005). SNAP-25, however, is not implicated in fusion pore formation or dilation, as we would expect from a protein lacking transmembrane domains. Synaptotagmin has been found to modulate the fusion pore (Wang et al., 2001; Wang and Sudhof, 2003). Analogous to chromaffin cells, the existence of a kiss-and-run mechanism of synaptic vesicles in neurons was proved: This process is much faster than the normal fusion of the synaptic cycle. The first clear indications for kiss-and-run fusion in synaptic boutons of hippocampal neurons were obtained by (Gandhi and Stevens, 2003).

After exocytosis, the empty synaptic vesicles are rapidly recovered through formation of clathrin coats and recycling through endosomal intermediates. The recycled vesicles fuse with early endosomes. Alternatively, recycling vesicles can form from membrane invaginations outside the active zone, through a clathrin-dependent mechanism, without undergoing endosomal intermediates. Empty vesicles just budded from the endosomes are filled with neurotransmitter by an electrochemical gradient created by a proton pump-driven, active transport. The translocation of refilled synaptic vesicles back to the active zone occurs either by diffusion or by transport along the cytoskeleton (Gandhi and Stevens, 2003).

2.3 Pools of synaptic vesicles

After leaving the depot pool of synaptic vesicles, the vesicles enter into the so called unprimed pool (UPP) and are docked to the plasma membrane (Ashery et al., 2000). Although the existence of an UPP in neurons is unclear (Rizzoli and Betz, 2005), there are numerous results, which support the existence of vesicles that are at the plasma membrane but are unable to fuse (Aravamudan et al., 1999; Augustin et al., 1999).

Docking was shown to be a reversible process in neurons and in neurosecretory cells (Oheim et al., 1998; Zenisek et al., 2000). In neurons, docking occurs only at the active zone. In the next step of the synaptic cycle, the vesicles have to undergo priming. The primed pool consists of two different vesicle pools: A slowly releasable pool (SRP) and a rapidly releasable pool (RRP). The RRP and SRP release at different rates, allowing estimation of pool size and kinetics using dual exponential fits, and they appear to be functionally separate pools of vesicles (Rettig and Neher, 2002). The two components of primed vesicles may result from different conformations of the SNARE complex, possibly stabilized to different degrees by interacting partners (such as synaptotagmin or complexin) (Rettig and Neher, 2002). A third, more slowly released sustained component, represents vesicles from the UPP, which undergo modifying steps, reach the primed state, and then fuse.

The size of the RRP in CNS synapses has been investigated using high frequency stimulation (Elmqvist and Quastel, 1965; Schneggenburger et al., 1999) and application of hypertonic sucrose (Rosenmund and Stevens, 1996). Based on these studies the RRP in CNS synapses most likely corresponds to the sum of SRP and RRP in chromaffin cells.

In adult chromaffin cells the depot contains about 20,000 vesicles. A total of about 850 morphologically docked vesicles is subdivided into the UPP (about 650 vesicles) and the primed pool, which is again subdivided into the SRP and RRP (each about 100 vesicles) (Rettig and Neher, 2002). Neurons of the CNS contain in each active zone about 170 vesicles in the reserve pool, about 20 vesicles in the

recycling pool and about 10 vesicles in the RRP (Rizzoli and Betz, 2005). Thereby the recycling pool corresponds more or less to the UPP, and the RRP to the sum of SRP and RRP in chromaffin cells.
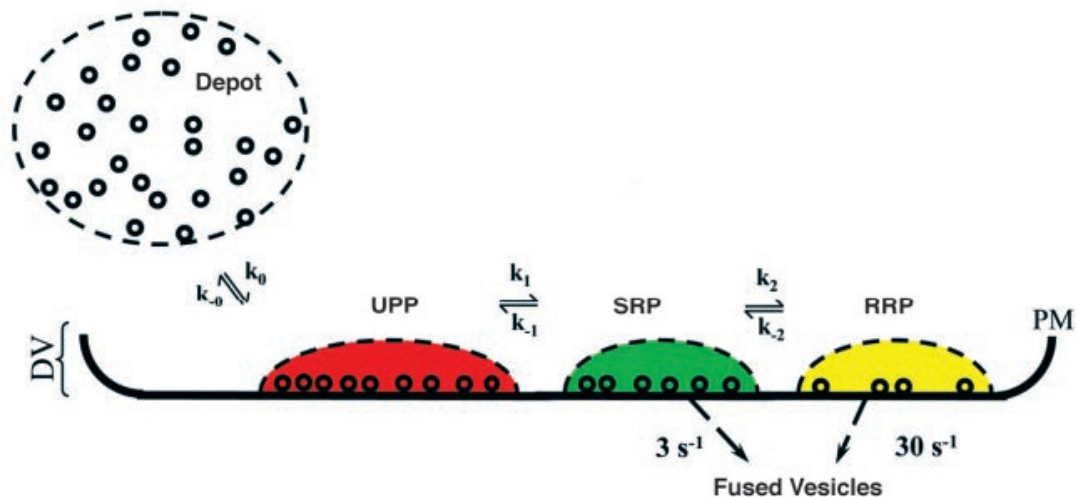
Figure 2.3: scheme of the 4 described vesicle pools at the presynapse (Rettig and Neher, 2002): RRP, SRP, UPP and vesicle depot. The vesicles of the depot pool enter the unprimed pool, UPP, when they dock at the membrane. After that they enter into the primed pool, with the latter again subdivided into the slowly releasable pool, SRP, and rapidly releasable pool, RRP. Thereby priming is defined functionally in the sense that all vesicles are termed `primed` if they can release within about a second of elevation of Ca^{2+} concentration. Primed vesicles are believed to be in one of the two states when they have at least partially assembled SNARE complexes.

2.4 SNARE proteins

The SNARE (soluble NSF attachment protein receptors) protein family consists of 3 subfamilies with homologues of Syntaxin, SNAP-25 (synaptosome-associated protein of relative molecular mass of 25 kD) and Synaptobrevin. Synaptobrevin is also called VAMP (vesicle associated membrane protein). This group of conserved proteins, which has more than 35 members in mammals, can be found in all eukaryotic fusion reactions and (Bock et al., 2001). SNARE proteins were independently discovered in yeast cells and neurons and were designated SNAREs since this complex is the specific target of NSF (N-ethylmaleinide-sensitive fusion protein) in conjunction with soluble NSF attachment protein (SNAP). The α-, β-, γ-SNAPs are not related to SNAP-25. The neuronal SNARE complex with

synaptobrevin (VAMP) on the vesicles- therefore they are also called v-SNARE –
and syntaxin1 and SNAP-25 on the target membrane – therefore also called t-
SNARE – has been well characterized (Jahn and Sudhof, 1999; Rizo and Sudhof,
2002).
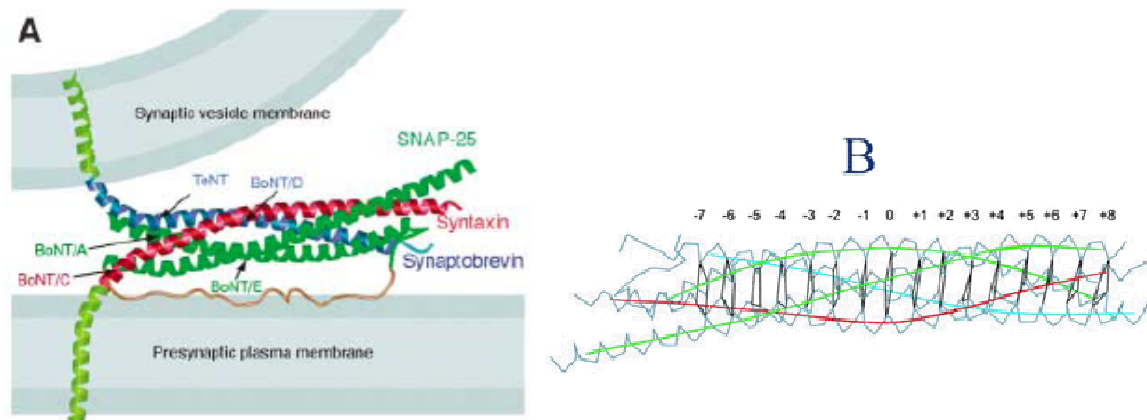
Figure 2.4: Structure of the neuronal SNARE complex(modified from Sakaba et al., 2005)
*A) Model of the neuronal SNARE complex containing synaptobrevin (VAMP) on the
   vesicles - therefore they are also called v-SNARE - and syntaxin1 and SNAP-25 on the
   target membrane - therefore also called t-SNARE.*
*B) The 4 α-helical bundles (coiled-coils) of the associated SNARE proteins form the so-
   called core complex containing 2 SNARE motifs from   SNAP-25 (green) and one each
   from synaptobrevin (blue) and syntaxin1 (red).*

The SNARE protein groups show little homology, but they all share one
homologous sequence, the SNARE motif, containing 60 – 70 amino acids with 8
heptad repeats. The 4 α-helix bundles (coiled-coils) of the associated SNARE
proteins form the so-called core complex containing 2 SNARE motifs from SNAP-
25 and one each from synaptobrevin and syntaxin1. Each helix adds one
hydrophobic residue to each layer – a leucine zipper-like layer consisting of 15
hydrophobic residues. An exception is the central zero-layer, which is ionic and
composed of 1 arginine (R) and 3 glutamines (Q). This led to the classification of
SNAREs as Q-SNARE – contributing glutamine – and R-SNARE – contributing
arginine. Both classifications of SNAREs are widely used. The complex is
extremely stable: it can not be denatured by heat or detergent in vitro and the only
way to dissociate in vivo seems to be the ATP-consuming NSF action (Jahn and
Sudhof, 1999).

The cleavage of SNAREs by the clostridial neurotoxins tetanus toxin (TeNT) and 7 botulinum toxins (BoNT/A – G) blocks neurotransmitter release. However, once the core complex is formed, it is resistant to cleavage by clostridial neurotoxins.

Differing from the initial 'SNARE-hypothesis', that mainly proposed a role of SNAREs in docking, it is now believed, that SNARE complexes play a role in membrane fusion (Chen and Scheller, 2001; Rizo and Sudhof, 2002) (see figure 2.5). To bring the vesicle and target membrane together the closed conformation of syntaxin needs to open to initiate core complex assembly. This process is caused by assembly of SNARE complexes in an N- to C-terminal zippering reaction during fusion without a stable, partially assembled intermediate (Matos et al., 2003).

The opposing membranes are pulled closer together (trans-complex). The transmembrane regions of the SNARE are present in the same membrane after fusion (cis-complex). NSF and SNAP to recycle SNAREs for another round of fusion catalyze the disassembly. Before fusion the trans-complex is believed to change from a loose into a tight state (Xu et al., 1999a). This could explain the presence of the SRP, reflecting the loose state, from which vesicles are able to fuse with slower rates. In this model the tight state would support the fast exocytosis from the RRP (Xu et al., 1999b; Rettig and Neher, 2002).
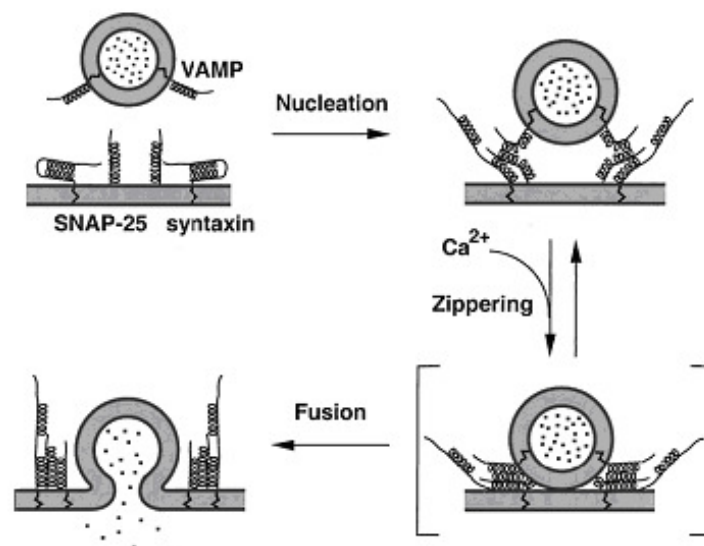
Figure 2.5: the synaptic cycle with the important steps of the 3 subfamilies proteins of the SNARE complex SNAP-25, syntaxin and synaptobrevin (VAMP) (reproduced from Lin and Scheller, 2000)

2.5 SNAP-25: a protein of the SNARE complex

As described in the previous chapter, SNAP-25 is a protein member of the SNARE complex. SNAP-25 is as well as syntaxin, located at the plasma membrane. Interaction of SNAP-25, syntaxin and synaptobrevin forms the SNARE complex. SNAP-25 was originally identified as a synaptosomal protein of 25 kDa which is expressed in nervous tissue (Oyler et al., 1989) and has been shown to exist in two variants (SNAP-25 A and B) (Bark et al., 1995). SNAP-25 is also expressed in adrenal chromaffin cells, insulin-responsive tissues (i.e. skeletal muscle) and clonal pituitary cells, which suggests that it may participate in stimulus-coupled secretion from nonneuronal cells (Roth and Burgoyne, 1994; Jagadish et al., 1996).

SNAP-25 possesses heptad repeats that have a high probability of forming α-helices and coiled coils. A putative coiled coil region located at the carboxyl terminus of SNAP-25 has been shown to mediate association with synaptobrevin and syntaxin (Chapman et al., 1994). Amino acids 150-206 of SNAP-25 form one of the four helices in the SNARE complex structure (Weimbs et al., 1997; Fasshauer et al., 1998).

Like synaptobrevin and syntaxin, SNAP-25 is cleaved by BoNT. Toxin treatment, which results in truncation of the carboxyl terminus, weakens the interaction between SNAP-25 and synaptobrevin in vitro and inhibits exocytosis from nerve endings (Chapman et al., 1994).

In addition to interactions with SNAREs, SNAP-25 interacts with the proposed calcium sensor in exocytosis, synaptotagmin, and has been suggested to bind to and regulate calcium channels (Rettig et al., 1996). These and earlier findings imply an additional regulatory role for SNAP-25 in the calcium-activated steps which lead to membrane fusion. In addition, SNAP-25 may be involved in the recycling process of synaptic vesicles (Walch-Solimena et al., 1995).

2.6 SGT: a molecular cochaperone at the presynaptic terminal

The SGT (small glutamine-rich tetratricopeptide repeat (TPR)-containing) protein was originally discovered because of its putative interaction with envelope proteins of two viruses, i.e., human immunodeficiency virus type 1 and parvovirus H-1 (Callahan et al., 1998; Cziepluch et al., 1998). A detailed sequence analysis revealed that SGT contains three tandem tetratricopeptide repeat domains (TPRs). The TPR domain is a degenerate 34 amino acid sequence found in a wide variety of proteins, present in tandem arrays of 3 to 16 motifs, which form scaffolds to mediate protein-protein interactions.

Many different roles of SGT have been suggested. One of the interaction factors for the human SGT is the growth hormone receptor (GHR) (Schantl et al., 2003). However, the biological importance of this interaction is still unknown. SGT plays an important role in cell division as well. In recent studies it was shown that human SGT is essential for successful completion of cell division (Winnefeld et al., 2004). In a Caenorhabditis elegans model for Alzheimer disease, which depends on induced exogenous expression of the intracellular β-amyloid peptide, SGT was found to be present in protein complexes and a depletion of SGT reduced the toxic effects of β-amyloid peptide expression, indicating a contribution of SGT protein to β-amyloid peptide-dependent pathogenicity in this model system (Fonte et al., 2002).

Additional interaction partner of the SGT protein are the heat shock cognate protein of 70 kDa (Hsc70) and the cystein string protein (CSP). These three proteins form a stable trimeric complex, which is located on the synaptic vesicle surface at the synaptic terminal and functions as a synapse-specific chaperone (Tobaben et al., 2001). The assembly of the trimeric complex is ADP-dependent, whereas ATP disassembles the complex. The Hsc70 ATPase is strongly activated by a combination of CSP and SGT, which points out the role of SGT as a cochaperone. The function of SGT as a ubiquitous cochaperone has been demonstrated (Angeletti et al., 2002). SGT binds to the C-terminus of Hsc70, a site used by several TRP-containing binding parterns to recruit Hsc70 into complexes

of diverse functions. It was shown that CSP functionally interacts with SGT in vivo and is required for the recruitment of SGT to the synaptic vesicles (Tobaben et al., 2001).
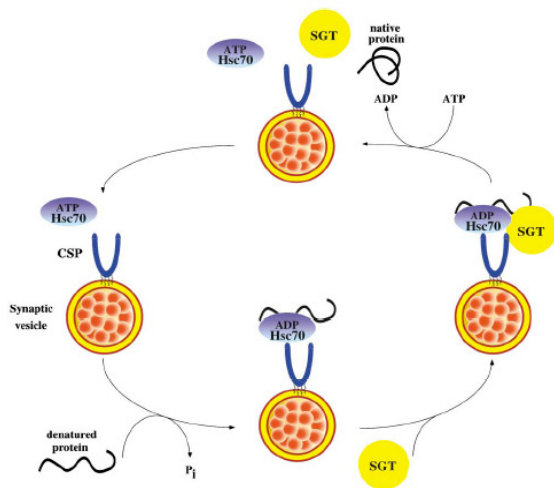
Figure 2.6: Model showing the cycle of the trimeric complex CSP/Hsc70/SGT on the synaptic vesicle (reproduced from Tobaben et al., 2001). The assembly of the trimeric complex is ADP-dependent, whereas ATP disassembles the complex. The Hsc70 ATPase is activated by a combination of CSP and SGT, which points out the role of SGT as a cochaperone.

Today there are two isoforms of SGT characterized: α-SGT and β-SGT. Whereas α-SGT is expressed ubiquitously, β-SGT is exclusively expressed in the brain and cooperates with α-SGT as a cochaperone of Hsc70 in the brain (Tobaben et al., 2003).

2.7 Motivation and aim of these projects

Although many presynaptic proteins have been identified, their role in neurotransmitter release is still not well understood.

The general aim of this project was to study the physiological role of SGT in hippocampal neurons. In addition I have examined the effects of the mutation of SNAP-25, SNAP-25Δ9, on neurotransmitter release in hippocampal neurons.

2.7.1 Studies of SNAP-25Δ9

In this project I used the mutant SNAP-25Δ9, in which the last nine C-terminal amino acids are missing (generated by Dr U. Matti, see (Wei et al., 2000), corresponding to the BoNT/A cleavage product. Overexpression of SNAP-25Δ9 - mutants in chromaffin cells leads to a selective reduction of the fast

component of the exocytotic burst in flash experiments while the size and the rate constant of the SRP remained unaffected, which can be explained by a destabilization and resulting reduction of the RRP (Wei et al., 2000). These results are in agreement with previous studies using BoNT to cleave endogenous SNAP-25 (Xu et al., 1998). In addition the SNAP-25Δ9 - mutation is thought to destabilise the C-terminal end of the SNARE complex during the zippering process (Sorensen et al., 2006).

Since there is still a disagreement about the existence of different vesicle pools in neurons, I wanted to investigate the kinetics of exocytosis in neurons and the effects of the SNAP-25Δ9 - mutation on this process, to attempt to distinguish between different pools in the releasable pool of neurons. Furthermore I wanted to determine if there was a difference in pool size between the Ca^{2+} dependent synaptic response induced by high frequency stimulation and the Ca^{2+} independent response induced by hypertonic sucrose solution in the SNAP-25Δ9 – mutation. A difference in the size of these two responses would indicate that different pools of vesicles are released by these two stimuli.

2.7.2 Studies of SGT

The knockout approach (SGT knockout mice were generated by the laboratory of Nils Brose (Max Planck Institute for Experimental Medicine, Göttingen, Germany) was used in order to investigate the physiological function of α-SGT and β-SGT in hippocampal neurons. Recent studies of the SGT protein demonstrate that overexpression of SGT in neurons leads to a reduction of pool size and also to a reduction of vesicular release probability (Tobaben et al., 2001).

In CSPα-lacking mice neither activity of Ca^{2+} channels nor exocytosis is significantly reduced. In spite of this the deletion of CSPα causes a progressive dysfunction of synapses, which is lethal at about 3-5 weeks of age. This phenomenon appears to be caused by a use-dependent loss of nerve terminal integrity and a dysfunction of the molecular trimeric complex of CSP/SGT/Hsc70 (Fernandez-Chacon et al., 2004). I wanted to determine

whether a similar phenomenon is present in SGT double knockout mice. To this end I have examined synaptic function in neurons from SGT double knockout mice after 1 to 4 weeks in culture using electrophysiological methods.

1. Material and Methods

3.1   Materials

3.1.1 General chemicals

Acetic Acid	Fluka
$CaCl_2$	Sigma
Creatinphosphate-Na	Sigma
EDTA	Sigma
EGTA-K	Sigma
Ethanol	Carl Roth
Formaldehyde	Sigma
Glucose	VWR International
GTP-Na	Sigma
HEPES	VWR International
KCl	VWR International
$MgCl_2$	VWR International
NaCl	VWR International
$NaH(PO_4)_2$	VWR International
NaH_2PO_4	VWR International
NGS	VWR International
Sp-cAMPs	VWR International
Sucrose	VWR International
Triton X-100	VWR International

3.1.2 Chemicals and media for cell culture

Agarose Type II A	Sigma
Albumin	Sigma
B27	Invitrogen
BSA	Sigma
Chloroform	Sigma
Collagen	Collaborative Biomedical Products
Cysteine	Sigma
DMEM (1x) with high glucose, sodium pyruvate and L-glutamine	Invitrogen
FCS (fetal calf serum)	Invitrogen
5-fluoro-2´-deoxyuridin	Sigma
Glycerin	Sigma
HBSS	Sigma
Hepes buffer 1M	Invitrogen
Mineral oil	Invitrogen
Neurobasal A	BD Biosciences

Papain	Worthington Biochemical Corporation
Penicillin/Streptomycin	Invitrogen
Phenol	Sigma
Poly-D-lysin	Sigma
Tris	Sigma
Trypsin-inhibitor	Sigma
Trypsin/EDTA solution	Invitrogen
Uridine	Sigma
Xylen cyanol FF	Sigma

3.1.3 Materials for cell culture

| Coverslips | VWR International |
| Culture plates, flasks, tubes, pipettes | VWR International |

3.1.4 Composition of cell culture media and solutions

1) NBA
100 ml Neurobasal-A, 2 ml B27-supplement, 1 ml Glutamax-stock, 200 µl Pen/Strep.

2) HBS
140 mM NaCl, 10 mM HEPES-NaOH, 5 mM KCl, 10 mM $MgCl_2$, 20 mM $CaCl_2$, pH= 7.3, 351 mOsm

3) PBS
140 mM NaCl, 7 mM KCl, 10 mM Na_2HPO_4, 1.8 mM KH_2PO_4

4) Enzyme solution
2 mg cystein, 10 ml DMEM, 0.1 ml $CaCl_2$ (100mM), 0.1 ml EDTA (50 mM), papain (17,5 units per ml of enzyme solution), bubbled with carbogen gas for 10-20 minutes

5) Inactivating solution
25 mg albumin, 25 mg trypsin-inhibitor, 10 ml 10%FCS-medium

6) Chymotrypsin
2 mg chymotrypsin in 1 ml HBS

7) Aprotinin
6 mg aprotinin in 1 ml HBS

8) Poly-D-lysin solution
1.2 ml acetic acid (17 mM), 0.4 ml collagen (0.5 mg/ml), 0.4 ml poly-D-lysin (0.5 mg/ml)

3.1.5 Experimental animal supply

1) SGT-mice	Dr. Guido Meyer, MPI Experimental Medicine, Göttingen, Germany
2) Wildtype mice	Animal house, Institute of Physiology, University of Saarland, Homburg, Germany

3.1.6 Virus

pSFV-GFP-SNAP-25Δ9	generated by Dr. Ulf Matti (Wei et al., 2000)

3.1.7 Chemicals, media and materials for PCR

Agarose for DNA electrophoresis	Roth
dH$_2$O	Sigma
λ-DNA marker EcoRI/hindIII	self made
Dneasy Tissue Kit	Qiagen
dNTPs (2.5 mM)	Fermentas
ethidium bromide	Roche
Electrophoresis system	PowerPac, Biorad
horizontal chamber for electrophoresis	Peqlab, Erlangen, Germany
Mastercycler Gradient	Eppendorf
phase advanced imaging system (UV-light = 312nm)	Phase, Lübeck, Germany
Primer#6115	Dr. Guido Meyer, MPI Experimental Medicine, Göttingen, Germany
Primer#2175	Dr. Guido Meyer, MPI Experimental Medicine, Göttingen, Germany
Primer#428	Dr. Guido Meyer, MPI Experimental Medicine, Göttingen, Germany
Primer#4182	Dr. Guido Meyer, MPI Experimental Medicine, Göttingen, Germany
Primer#4183	Dr. Guido Meyer, MPI Experimental Medicine, Göttingen, Germany
RedTaq-DNA-Polymerase	Sigma
RedTaq PCR-Buffer	Sigma
TAE with 40 mM Tris, 0.11% (v/v) Acetic acid, 1 mM EDTA, pH= 8.0	self made

3.1.8 Patch-clamp set up

Borosilicate glass GB 150 F 8P	Science Products GmbH, Hofheim
EPC-9 patch clamp amplifier with PULSE software package	HEKA Electronics
Electrical micromanipulator with head stage	Eppendorf
Faraday cage	Workshop, MPI Biophysical Chemistry, Göttingen, Germany
Fast flow system SF-77B	Warner Instrument Corporation
Glass tubing for flow pipes	Polymicro Technologies
Computer	medvis (PC)
Axiovert-10 Zeiss inverted microscope	Zeiss
Metamorph software	Molecular Devices Corporation, Sunnyvale, USA
Microforge	World Precision Instruments
Micropipette puller	Sutter Instruments Company and TSE System
Monochromator	General Scanning
Monitor (bw)	Panasonic
Oscilloscope	Philips
Perfusion system with	Workshop, MPI Biophysiocal Chemistry, Göttingen, Germany
exhaust pump	Wisa, Aqua United, Telgte, Germany
Photometric Set-up with	T.I.L.L. Photonics
CF 14 camera	Kappa Messtechnik, Gleichen, Germany
Piezoelectric micromanipulator	HEKA Electronics
Vibration isolation table	Newport

3.1.9 Solutions for electrophysiology experiments

1) extracellular physiological saline (Base + 10x) in mM
140 NaCl, 24 KCl, 100 HEPES, 40 $MgCl_2.6H_2O$, 40 $CaCl_2.2H_2O$, 100 glucose, pH= 7.3, adjusted with NaOH, 300 mOsm

In the case of hypertonic sucrose solution, 500mM sucrose was added to the normal extracellular physiological solution (Base + 1x)

2) intracellular (pipette) solution in mM
136 KCl, 17.8 HEPES, 0.6 $MgCl_2$, 4 ATP-Mg, 0.313 GTP-Na_2, 15 creatinphosphate, 1 K-EGTA, pH= 7.45, 290 mOsm

3.2   Methods

3.2.1 Knockout mice

Deletion mutations in the mouse gene for α/β SGT were generated by Guido Meyer. Heterozygous α/β SGT mice (male and female) were provided by the laboratory of Nils Brose (Guido Meyer, MPI Experimental Medicine Göttingen, Germany). The heterozygous SGT-mice were paired to obtain the homozygous wild type and double-knockout mice.

3.2.2 Genotyping of mice

3.2.2.1   Preparation of mouse genomic DNA

For digestion of mouse tails and purification of DNA the Dneasy Tissue Kit (Cat. No 69506) from Qiagen, Hilden, Germany with the protocol for rodent tails was used.

3.2.2.2   Polymerase chain reaction (PCR)

With PCR it is possible to duplicate selectively any parts of a nucleic acid sequence from a DNA template in vitro. In my case a two primer PCR for each SGT-protein and each genotype was used for genotyping. In the α-wild type reaction, Primer #2175 and #6115, and in the α-knockout reaction, Primer #428 and #6115 were used respectively, in the case of β-SGT, Primer #4182 and #4183 for wild type reaction, and Primer #428 and #4182 for knockout reaction were used. For each wild type and knockout allele only one PCR product is observed on the gel. For the α-wild type allel a 1.6 kb amplicon is generated whereas for the α-knockout a 1.5 kb amplicon accumulates. For the β-wild type allele, a 280 bp, and for the β-knockout allele, a 250 bp amplicon is generated. If the DNA derives from a heterozygous mouse both primer pairs can form an amplicon, since both alleles, knockout and wild type, are present.

Primer # 6115: GGA GCC ACA CGT GGC CTG C

Primer # 2175: CAC TTG GGA GGC ATA GGC AGA TGG

Primer # 428: GAG CGC GCG CGG CGG AGT TGT TGA C

Primer # 4182: CAA GGG TGA TTC TCC ATA TGT C

Primer # 4183: ATA ACA AGG GTC ATC CAC CA

For the PCR a mastermix with following ingredients for each SGT-protein was used:

1 μl DNA template

1 μl dNTPs   (2.5 mM)

1 μl Primer#   (5 pmol/μl)

1 μl Primer#   (5 pmol/μl)

1 μl RedTaq-DNA-Polymerase

2 μl RedTaq PCR-Buffer

13 μl dH$_2$O

The cycling program started with 5 min at 95°C (initial denaturation) followed by 35 cycles of 30 sec at 94°C, 30 sec at 60°C and 60 sec at 72°C; final extension for 10 min at 72°C and then hold at 4°C. A Mastercycler Gradient from Eppendorf, Hamburg, Germany was used.

3.2.2.3   Agarose gel electrophoresis for DNA separation

For separation of DNA fragments of different lengths, agarose gels were used. The necessary amount of 2% agarose (w/v) was boiled using a microwave. After cooling to 50°C, 2 μl ethidium bromide per 30 ml was added (final concentration 0.5 μl/ml). The agarose was put into a horizontal chamber for electrophoresis (Peqlab, Erlangen, Germany) and chilled at room temperature until the gel was solid. The chamber was then filled with 1xTAE buffer. DNA probes were put into gel pockets. The first gel pocket was filled with λ-DNA Marker as standard. Electrophoresis was performed at 80 V for 45 minutes (PowerPac, Biorad). Due to the intercalation of ethidum bromide, DNA fragments were visible as stripes

under UV-light (312 nm). For documentation the phase advanced imaging system was used (Phase, Lübeck, Germany).

3.2.3 Preparation of hippocampal neurons in micro-island culture

3.2.3.1 General

Synapses of cultured hippocampal neurons are well suited for studying synaptic transmission. When the axon of a hippocampal neuron is forced to grow in culture, its axon will form synapses with its cell body – called autapse. A large number of autaptic connections are formed. Using such micro-island cultures of single hippocampal neurons (Fig. 3.1) the autaptic origin of all synapses can be confirmed. There cultures are suitable for estimates of quantal size (Bekkers and Stevens, 1991).
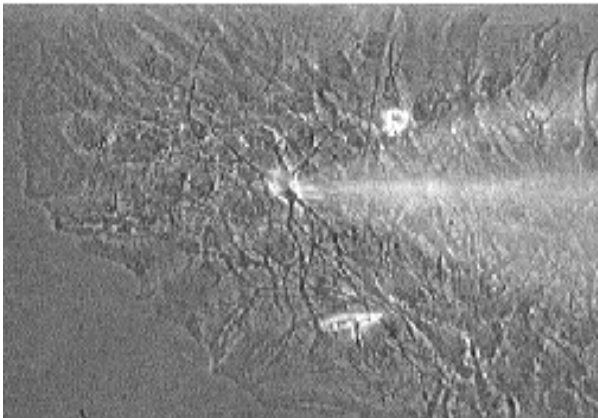
Figure 3.1: A neuron in a micro-island culture.
The neuron is growing on a small `island` of the substrate on which astrocytes have colonized. The patch pipette is out of focus and is approaching from the right side of the picture.

Using the patch pipette the neuron can be stimulated which results in synaptic neurotransmitter release at the autapses. The response to this autaptic release can also be recorded via the same patch pipette. From these measurements of EPSCs and IPSCs, the parameters such as kinetics, pharmacological properties, and quantal size can be calculated.

3.2.3.2 Preparation and cell-culture

The preparation of the hippocampal neurons in micro-island culture was performed according to a procedure modified from Bekkers and Stevens (1991).

Therefore 30 mm diameter glass coverslips were used. The coverslips were rinsed several times with 70% ethanol and stored in 95% ethanol until used. To make the micro-island cell culture, 1.5% agarose solution was spread thinly on the flame dried coverslips. Micro-dots of a mixture of collagen and poly-D-lysine were applied on air dried agarose coated coverslips using a stamp containing regularly spaced squares of 200 x 200 µm. The culture plates were then sterilized by UV radiation for 30 minutes. Micro-island of astrocyte feeder cells was prepared 2-3 days before plating the neurons.

Astrocytes and neurons were obtained from mice that were decapitated at P1 to P2, according to the rules of the state and animal welfare committee.

For primary cultures of astrocytes the hippocampus was dissected out of the brain and removed in physiological Hank Balanced Salt Solution (HBSS). The hippocampus tissue was cleaned of meninges and vascular tissues and then dissociated either enzymatically in solution containing 35 units papain/2ml or mechanically by passing through a 100 µm nylon cell trainer. About 580K (K= 1000) of dissociated astrocytes were grown in 75 cm² flasks in DMEM medium containing 10% fetal calf serum (FCS) in an incubator maintained at 5% CO_2 and 37°C. When the astrocytes were 70-80% confluent, splitting was carried out by incubation with trypsin (0.05%)-EDTA (0.02%) solution. The enzymatic action of trypsin was stopped by 10% FCS. The astrocytes were then seeded on the previously made micro-islands in the concentration of 35K and allowed to grow further for 4-5 days until a monolayer of cells was obtained. Further proliferation of the astrocytes was inhibited by addition of 10 µm 5-fluoro-2´deoxyuridine.

To obtain hippocampal neurons, the hippocampi were taken out of the brain, and cleaned in HBSS and enzymatically dissociated with papain solution containing 35units/2ml for 30 minutes at 37°C with gentle agitation. The enzymatic action of papain was stopped by an inactivating solution containing albumin and trypsin-inhibitor in 10% FCS-medium. To make a suspension of dissociated neurons, loosely bound hippocampal tissue was carefully triturated with an Eppendorf pipette. Before plating the hippocampal neurons on the astrocytes, the medium of

the astrocytes-plates was replaced with serum-free Neurobasal A medium supplemented with B27. The neurons were plated at the density of 4K per well. The neuron-cultures were allowed to grow at least 8 days in an incubator at 37°C and with 5% CO_2, at which time autapses were present.

3.2.4 Transfection of hippocampal neurons

3.2.4.1   General

With the help of the overexpression method based on the Semliki Forest virus (SFV) it is possible to express exogenous proteins and to test their properties in hippocampal neurons. SFV has a capped, polyadenylated single- stranded RNA genome, which functions as a mRNA in infected cells. The gene of interest can be directly ligated to a DNA cloning vector encoding nonstructural SFV genes for replicase, reverse transcriptase and helicase. Green fluorescent protein (GFP) from Aquorea victoria (Prasher et al., 1992) was used as a transformation marker to detect the overexpression of the protein. In neurons, overexpressed proteins can be detected 3-4 hours after infection with the virus and they appear to be targeted to their proper functional sites. The efficiency of SVF-mediated overexpression is very high, and a substantial overexpression can be detected within a reproducible time window, although SFV infection causes cell death ultimately. The subcellular organization of infected hippocampal neurons is maintained at least 16 hours post infection. After 24 hours morphological changes become apparent (Olkkonen et al., 1993; Weclewicz et al., 1998; Ashery et al., 1999). Furthermore, infected cells maintain their electrophysiological properties such as a low intracellular Ca^{2+} concentration, estimable Ca^{2+} currents and evoked release (Ashery et al., 1999).

3.2.4.2   Infection with pSFV-GFP-SNAP-25Δ9

Frozen vials of pSFV-GFP-SNAP-25Δ9 (450 µl) containing cDNA of the respective proteins coupled with GFP were thawed to room temperature and diluted 1:1 v/v with conditioned medium from the neuronal culture. To activate

the virus, 100 µl chymotrypsin was added and incubated at room temperature for 45 minutes. The chymotrypsin activity was stopped by addition of 110 µl aprotinin and further incubation of the virus for 10 minutes. 25-35 µl from an activated virus was added to the wild type neuronal plates and the plates were returned to the incubator at 37°C and 5% CO_2. Protein expression was determined for electrophysiological experiments 5-7 hours after infection as the appearance of green fluorescence - due to expression of GFP and detectable by photometric set-up (T.I.L.L. photonics) with camera (Kappa Messtechnik, Gleichen, Germany) and Metamorph software (Molecular Devices Corporation, Sunnyvale, USA). A comparison of control and infected neurons is shown in figure 3.2.
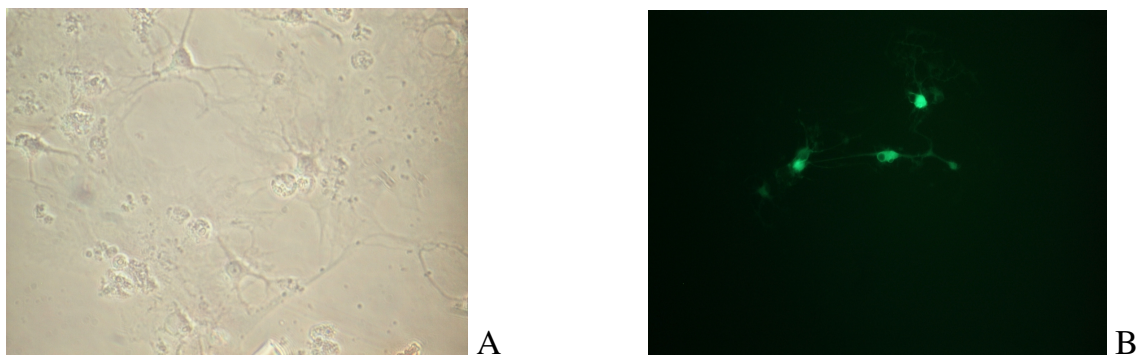
Figure 3.2: Neurons in cell culture
A) Phase contrast micrographic picture of a neuronal cell culture at day P10 in cell culture with 200x magnification with an inverted microscope
B) The same neuronal cell culture shown in A) 6h after the infection with the Virus pSFV-GFP-SNAP-25Δ9. Green fluorescence results from illumination of the culture with light of the wavelength 485 nm due to the presence of the GFP (green fluorescent protein) in the viral construct. Neurons exhibiting green fluorescence are virus infected and are expressing SNAP-25Δ9.

3.2.5 Electrophysiology

3.2.5.1 Patch clamp technique

The patch clamp technique was initially developed to measure single ion channel currents (Neher and Sakmann, 1976). To record these very small currents, low background conductance is a major requirement, which is met by the formation of a high resistance seal between the pipette tip and the cell. Under microscopic

control the patch pipette is gently placed onto the cell and "sealed" to the plasma membrane by application of light suction. During this procedure the resistance between pipette tip and cell membrane reaches some Giga Ωs.

The commonly employed ´whole cell´ configuration (Hamill et al., 1981) is obtained by initially establishing a Giga-seal and then rupturing the patch underneath the pipette tip with a stronger pulse of suction. In the whole cell mode, the soma can be ´voltage clamped´ allowing measurements of the currents caused by exocytically released glutamate. The neuron can be depolarised with a short depolarisation, which results in an action potential, which proceeds over the axon to the terminal ending of the neuron resulting in release of transmitter. Since the synaptic terminals target the dendrites of the same cell, one can also record the synaptic currents (EPSCs) resulting from the depolarisation.

In the voltage clamp mode the membrane potential V_m is held constant at about -70 mV while the current flowing through the membrane is measured. In this mode by brief depolarisation at the soma at a low frequency (e.g. 0.2 Hz) the basic scheme of synaptic transmission can be elicated as EPSCs or IPSCs of autaptic currents in isolated hippocampal neurons (Bekkers and Stevens, 1991).

With a high frequency (e.g. 20 Hz) the short term synaptic depression with high probability of transmitter release can be generated (Zucker, 1989; Zucker and Regehr, 2002). This depression has generally been attributed to depletion of the pool of readily releasable vesicles (Takeuchi, 1958; Thies, 1965; Betz, 1970; Wu and Borst, 1999).

All patch clamp experiments were carried out routinely on day P8 – P14 and in case of SGT on P21 – P24, too. Extracellular physiological solution was freshly made from stock solution. Fresh aliquots of intracellular solution were used on each new day. The pH and osmolarity of the required solutions were checked regular. In case of the sucrose-experiments normal extracellular solution made hypertonic by addition of 500 mM sucrose was used.

The patch pipettes were prepared from borosilicate glass GB 150 F 8P, pulled with a Sutter Instruments Company pipette puller and also with a TSE system pipette puller.

3.2.5.2 Fast application system

The RRP size in hippocampal neurons can be determined by application of hypertonic sucrose solution (normal extracellular solution made hypertonic by addition of 500 mM sucrose) for 3-5 sec. The treatment with hypertonic solution evokes a transient inward current that is followed by a steady current component. A fast-flow system that allows a rapid application and exchange of external solutions can be used to apply a pulse of the hypertonic sucrose solution. The hypertonic solution is applied to the single neuron in micro-island cultures in such a way, that the entire dendritic tree is exposed to the sucrose solution (Figure 3.3). The integral of the sucrose-current upon hypertonic sucrose application provides a measure of the size of the releasable vesicle pools.
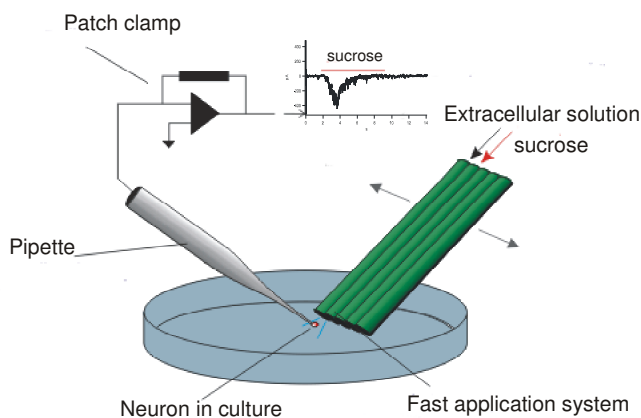
Figure 3.3: Fast application system (modified to http://www2.biomed.cas. cz/d331/eng/glutamate_en g/glutamat_apl_eng.html)

The exact mechanism of release mediated by hypertonic solution is not known. It is a Ca^{2+} independent mechanism (Blioch et al., 1968; Quastel et al., 1971; Shimoni et al., 1977), partially mediated by the high osmolarity, which causes a shrinking of the cells. This is accompanied by rapid release of releasable synaptic vesicles. The release may be caused by mechanical stress on the integrins which link ligands in the extracellular matrix with the active zone structures in the terminals, with a probable contribution of intracellular Ca^{2+} stores (Stevens and Tsujimoto, 1995; Rosenmund and Stevens, 1996; Kashani et al., 2001). Finally these mechanisms cause the transmitter release at the synaptic terminal.

3.2.5.3   Protocol for the examination of the protein SNAP-25Δ9

To examine the effect of SNAP-25Δ9, the neurons were stimulated (depolarisation to +10 mV for 2 ms) in the voltage clamp mode with a low frequency (0.2 Hz) to determine the EPSC characteristics and to establish a baseline response for later comparison with responses to stimulation. After 20 stimuli of 0.2 Hz the cells were stimulated by hypertonic sucrose solution for 6 seconds with the fast application system, followed by 20 stimuli of 0.2 Hz again, and finally a fast train stimulation of 50 stimuli at 20 Hz – to check the Ca^{2+} dependent vesicle release -, followed by a second stimulation of hypertonic sucrose solution during 6 seconds with the fast application system, and at the end a recording of 20 stimuli of 0.2 Hz.

3.2.5.4   Protocol for the examination of the protein SGT

To examine the effect of SGT, the neurons were stimulated (depolarisation to +10 mV for 2 ms) in the voltage clamp mode with a low frequency (0.2 Hz) to determine the EPSC characteristics and to establish a baseline response for later comparison with responses to stimulation trains. After 20 stimuli of 0.2 Hz the cells were stimulated by 50 stimuli of 20 Hz, 20 stimuli of 0.2 Hz, 30 stimuli of 50 Hz, again 20 stimuli of 0.2 Hz and finally they were stimulated by hypertonic sucrose solution during 6 seconds with the fast application system. With this protocol is was possible to determine the characteristics of EPSCs, the short term depression in case of different high frequency stimulations and the vesicle pool size of the neurons.

3.2.6 Statistical analysis

Only measurements with stable series resistance between 7-15 MΩ and a leak current up to 1/10th of the recorded current were considered for the analysis.
The experimental data were imported into IGOR Pro (Wave Metrics, Lake Oswego, USA). Macros written by Dr. Detlef Hof, Institute of Physiology, University of Saarland, Homburg, Germany were used for the analysis.

The action potential-dependent release was quantified as the peak of EPSCs from the baseline value. EPSC amplitudes at high frequency stimulation were calculated as peak amplitude and then normalised to the last 4 responses of the previous 0.2 Hz stimulation before (stable state). The normalised EPSC amplitudes with the corrected baseline were then plotted as a function of time to analyse the depression during the high frequency stimulation train. For quantifying the kinetics of depression the curves were fitted with two time-constants, τ_{slow} and τ_{fast}, with following two exponentional equation: $f(t) = A_0 + A_{fast} * (1 - \exp(-(t-T_0)/\tau_{fast})) + A_{slow} * (1 - \exp(-(t-T_0)/\tau_{slow}))$. τ_{fast} presents the rapid decay component of neurotransmitter release and τ_{slow} the slow decay component. τ_{fast}, τ_{slow} and the steady state at the end of the depression, y_0, were compared.

The size of the vesicle pool of synaptic vesicles was determined from the integral of the total charge transfer on application of hypertonic sucrose.

The data were expressed as mean ± standard error of the mean and the statistical significance was tested using Two-paired Student's t-test and Mann-Whitney-U Ranking test with Sigma Stat Software (SPSS Inc, Chicago, USA).

4. Results

4.1 Overexpression of SNAP-25Δ9

I have examined synaptic transmission on SNAP-25Δ9 - overexpressing neurons to determine whether the presence of this mutant leads to changes in neurotransmitter release. So I compared responses to high frequency stimulation of hippocampal cell autapses in wildtype and SNAP-25Δ9 - overexpressing neurons. I also compared release induced by hypertonic sucrose solution before and after high frequency stimulation in these cells groups. The aim of these experiments was to investigate the different kinetics of the neurotransmitter release in hippocampal neurons. Second, I wanted to prove a difference between the Ca^{2+} dependent synaptic response induced by high frequency stimulation and the Ca^{2+} independent response induced by hypertonic sucrose solution in SNAP-25Δ9 - mutants to investigate whether the same vesicle pools are released in case of hypertonic sucrose solution application and of Ca^{2+} dependent neurotransmitter release.

4.1.1 Effect of SNAP-25Δ9 - overexpression on EPSC amplitude

EPSC amplitude was detected in hippocampal neurons overexpressing the SNAP-25Δ9 mutant and compared to that in wildtype hippocampal neurons. EPSCs were recorded during 0.2 Hz stimulation under voltage-clamp mode. The mean of EPSC amplitude was calculated as the mean of each cell during 0.2 Hz stimulation (20 stimuli). The mean of wildtype cells was 2.02 ± 0.187 nA, n= 35, and of SNAP-25Δ9 - overexpressing neurons, 1.7 ± 0.213 nA, n= 39. There was no significant difference between theses two groups, p= 0.267.
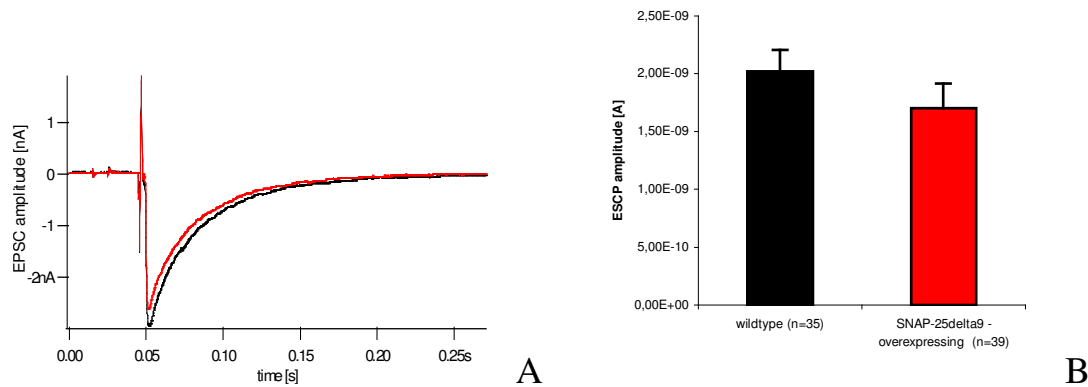
Figure 4.1.1:
A) exemplary traces of EPSC recording of wildtype (black) and SNAP-25Δ9 - overexpressing neuron (red).
B) mean and SEM of EPSC amplitudes of wildtype (black, n= 35) and SNAP-25Δ9 overexpressing neurons (red, n= 39). The mean of wildtype cells was 2.02 ± 0.187 nA, n= 35, and of SNAP-25Δ9- overexpressing neurons, 1.7 ± 0.213 nA, n= 39, p= 0.267.

4.1.2 Effect of SNAP-25Δ9 - overexpression on vesicle pool size

In order to test whether the pool size of SNAP-25Δ9 - overexpressing neurons is altered, the pool size was determined. The currents induced by a 5 s long application of hypertonic sucrose solution, which leads to a Ca^{2+} independent release (Rosenmund and Stevens, 1996), were measured. Exemplary traces of electrophysiological responses of sucrose treatment are shown in figure 4.1.2 . I also investigated whether high frequency stimulation reduced the pool size compared to the pool I measured before by application of hypertonic sucrose solution. Therefore I compared the response to hypertonic sucrose solution before and after high frequency stimulation: I stimulated with hypertonic sucrose solution, after 0.2 Hz stimulation (20 stimuli) and then applied a second sucrose stimulus after 20 Hz stimulation (50 stimuli). The integral of charge transfer during hypertonic sucrose application was analysed as an estimate of the total pool size.

Application of hypertonic solution produces a visible decrease in the volume of neuron cell bodies, of the neuronal dendrites and of the axons in the region of application. Therefore, the release of neurotransmitter is more likely mechanical induced by shrinking of the cells and not Ca^{2+} dependent.

Sucrose application
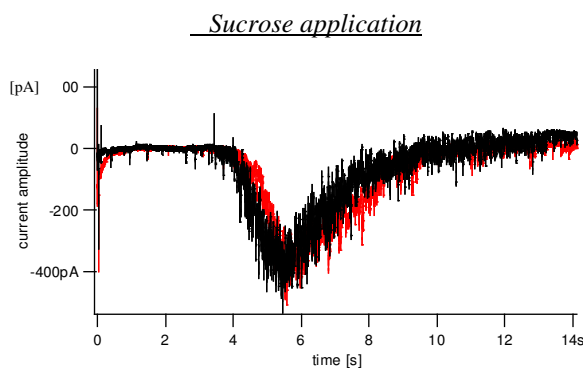
Figure 4.1.2: exemplary normalised traces of hypertonic sucrose solution application for wildtype (black) and SNAP-25Δ9 – overexpressing neurons (red)

As seen in the case of synaptically evoked responses, postsynaptic currents induced by application of hypertonic sucrose solution were also not reduced to a comparable degree (Fig. 4.1.3A and Fig.4.1.4A). The mean of total charge transfer during the first sucrose application after 0.2 Hz stimulation was 0.958 ± 0.288 nC, n= 25, for control cells and 0.573 ± 0.103 nC, n= 31, for SNAP-25Δ9 - overexpressing cells, p= 0.479. The mean of total charge transfer during the second sucrose application after 20 Hz stimulation was 0.643 ± 0.175 nC, n= 23, for control cells and 0.436 ± 0.089 nC, n= 24, for SNAP-25Δ9 – overexpressing cells, p= 0.333 (Fig. 4.1.3B and Fig. 4.1.4. B). The observed results showed no significance. Thus, the pool size of released vesicles was not reduced by overexpression of SNAP-25Δ9.

There was a slight but insignificant reduction in the response after the application of hypertonic sucrose solution after low frequency stimulation with 0.2 Hz as compared to the sucrose application after high frequency stimulation with 20 Hz for wildtype. The first stimulation for wildtype was noted as 0.958 ± 0.288 nC, n= 25, and the second stimulation was noted as 0.643 ± 0.175 nC, n= 23, p= 0.577. For SNAP-25Δ9 – overexpressing neurons the first stimulation resulted in a charge release of 0.573 ± 0.103 nC, n= 31, while the second stimulation released 0.436 ± 0.089 nC, n= 24, p= 0.420. The slight reduction of response in the second sucrose application after high frequency stimulation corresponds to short-term depression of EPSCs after high frequency stimulation as reported previously (Rosenmund and Stevens, 1996).

There was no significant reduction of vesicle pool size in the experiments using SNAP-25Δ9 – overexpressing neurons.
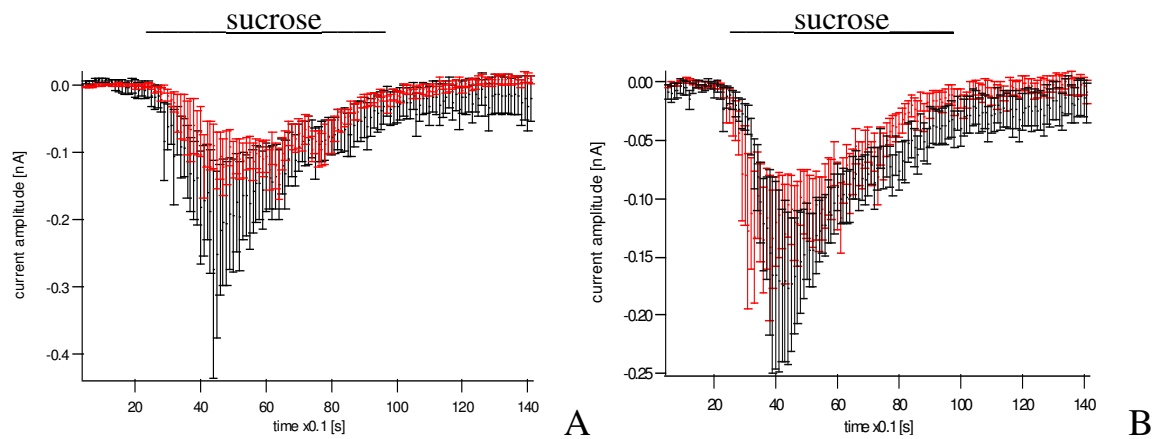
Figure 4.1.3:
A) Average and SEM of sucrose application after low frequency stimulation with 0.2 Hz from wildtype neurons (n= 25; black) and SNAP-25Δ9 – overexpressing neurons (n= 31; red). Data are normalised to the baseline of 0 nA.
B) Average and SEM of sucrose application after high frequency stimulation with 20 Hz from wildtype neurons (n= 23; black) and SNAP-25Δ9-overexpressing neurons (n= 24; red). Data are normalised to the baseline of 0 nA.
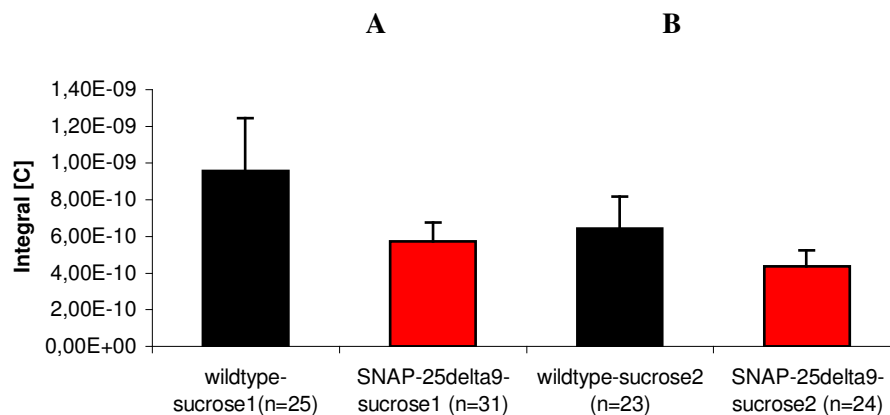
Figure 4.1.4: mean and SEM of the integral of sucrose application
A) sucrose application after low frequency stimulation with 0.2 Hz; mean of total current transfer during the first sucrose application was 0.958 ± 0.288 nC, n= 25, for control cells and 0.573 ± 0.103 nC, n= 31, for SNAP-25Δ9 – overexpressing cells, p= 0.479.
B) sucrose application after high frequency stimulation with 20 Hz; mean of total current transfer during the second sucrose application was 0.643 ± 0.175 nC, n= 23, for control cells and 0.436 ± 0.089 nC, n= 24, for SNAP-25Δ9 – overexpressing cells, p= 0.333.

4.1.3 Recovery after sucrose stimulation

We determined the recovery of the vesicle pool after release induced by application of hypertonic sucrose solution. We analysed the relationship between the recovery EPSCs after sucrose application and the pretrain EPSCs. Therefore the mean and SEM of the amplitude of the last 4 EPSCs of 0.2 Hz stimulation before sucrose application were used as the baseline and compared with the EPSC amplitude after sucrose application for each cell. Data are presented in figure 4.1.5.
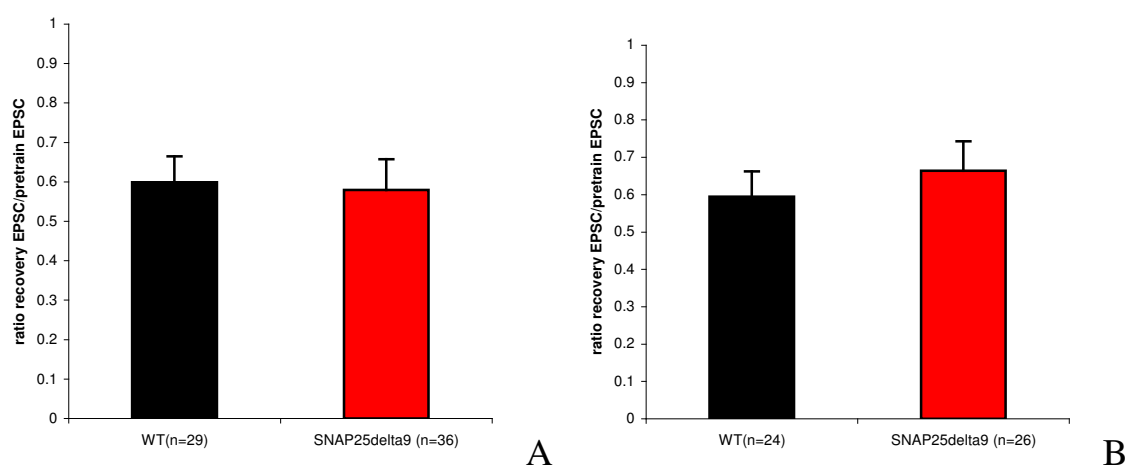
Figure 4.1.5 :
A) mean and SEM of ratio of recovery EPSCs to prestimulation EPSCs after first sucrose stimulation for wildtype neurons (n= 29) was 0.598 ± 0.065 and for SNAP-25Δ9–overexpressing neurons (n= 36) 0.579 ± 0.077, p= 0.387.
B) mean and SEM of ratio of recovery EPSCs to prestimulation EPSCs after second sucrose stimulation was 0.595 ± 0.067 for wildtype (n= 24) and 0.664 ± 0.079 for SNAP-25Δ9 – overexpressing neurons (n= 26), p= 0.641.

After the first application of hypertonic sucrose solution the mean and SEM of the ratio of recovering EPSC amplitude to prestimulus EPSC amplitude for wildtype neurons (n= 29) was 0.598 ± 0.065 and for SNAP-25Δ9–overexpressing neurons (n= 36) 0.579 ± 0.077. The mean and SEM of the second sucrose application was 0.595 ± 0.067 for wildtype (n= 24) and   0.664 ± 0.079 for SNAP-25Δ9–overexpressing neurons (n= 26). There was no significant difference between these different control groups: p= 0.387 for the ratio of recovery after the first sucrose stimulus and p = 0.641 for the ratio of recovery after the second sucrose stimulus.

Generally the recovery of the presynaptic vesicles pools was not reduced in SNAP-25Δ9 – overexpressing neurons after hypertonic sucrose solution application.

4.1.4 Effect of SNAP-25Δ9 - overexpression on short-term synaptic depression

In order to investigate changes in short-term synaptic plasticity, a high frequency stimulation protocol (50 stimuli at 20 Hz) for 2.5 s was carried out on wildtype and SNAP-25Δ9 – overexpressing neurons. With this protocol we could differentiate between the Ca^{2+} dependent neurotransmitter release during 20 Hz stimulation and the Ca^{2+} independent release induced by application of hypertonic sucrose solution, which was not reduced in SNAP-25Δ9 – overexpressing neurons. The resulting EPSC amplitudes were normalised to the value of the last 4 responses at 0.2 Hz serving as the baseline during the entire examination. The depression curves were plotted as a function of time.
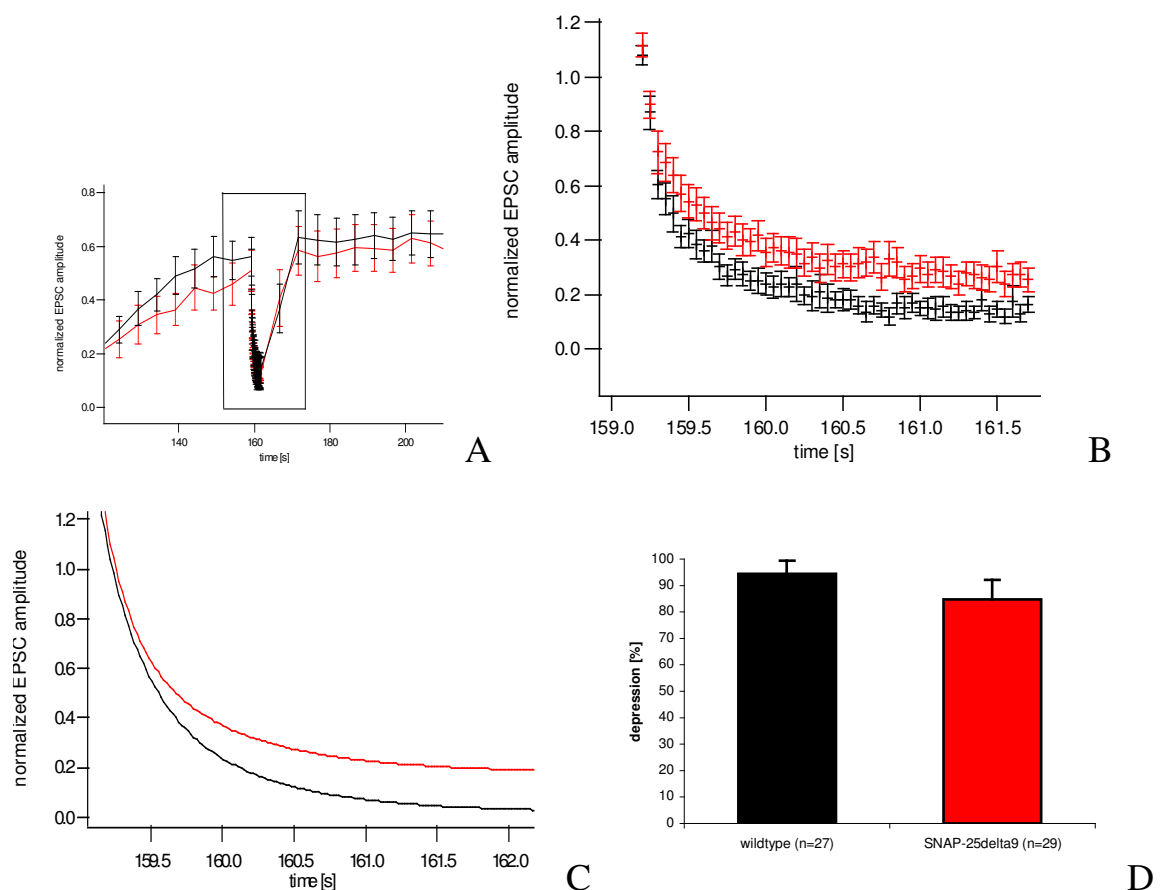
Figure 4.1.6:
A) average of the cell-recordings during 0.2 Hz stimulation at the beginning, 20 Hz stimulation and finally 0.2 Hz stimulation for wildtype (n= 32, black) and SNAP-25Δ9 - overexpressing neurons (n= 32, red). The 20 Hz stimulation is boxed.
B) enlarged section of the boxed region in A: average of wildtype (n= 28; black) and SNAP-25Δ9 – overexpressing neurons (n= 29; red) during 20 Hz stimulation (50 stimuli). EPSC amplitudes were normalised to the value of the last 4 responses of 0.2 Hz, which served as baseline during the whole experiments on these cells. The depression curves were plotted as a function of time.
C) average of fitted curves of wildtype (black; n= 27) and SNAP-25Δ9 – overexpressing cells (red; n= 29). There was no significant change of the kinetics but of the steady state y_0 (p= 0.015).
D) depression of wildtype (n= 27; black) and SNAP-25Δ9 – overexpressing neurons (n= 29; red), p= 0.015.

As predicted from previous data of SNAP-25Δ9 mutants in chromaffin cells (Wei et al., 2000; Sorensen et al., 2006) and of previous studies using BoNT to cleave endogenous SNAP-25 (Xu et al., 1998), SNAP-25Δ9 - overexpressing neurons show a slower depression curve and a reduced pool depletion.

To obtain more detailed information about the kinetics of pool depletion double-exponential fits were applied to both control and overexpression data. These data for 20 Hz trains are shown in the Table 4.1.1:

	fast component (τ_{fast})	slow component (τ_{slow})	steady state (y_0)
wildtype neurons (n= 27)	0.256 ± 0.061s	0.735 ± 0.231s	0.057 ± 0.051s
SNAP-25Δ9 – overexpressing neurons (n= 29)	0.196 ± 0.032 s	0.740 ± 0.119 s	0.154 ± 0.076 s

Table 4.1.1: summary of the fitted data of 20 Hz stimulation (values are given as mean ± SEM [s])

The rate of pool depletion was similar in these two groups. τ_{fast} was 0.256 ± 0.061s, n= 27, for wildtype and 0.196 ± 0.032 s, n= 29, for SNAP-25Δ9 – overexpressing

neurons, p= 0.658. τ_{slow} was 0.735 ± 0.231s, n= 27, for wildtype and 0.740 ± 0.119 s, n= 29, for SNAP-25Δ9 – overexpressing neurons, p= 0.201.

The steady state y_0 was significantly increased for SNAP-25Δ9 – overexpressing neurons, 0.154 ± 0.076 s, n= 29, compared to wildtype cells, 0.057 ± 0.051s, n= 27, p= 0.015. This result shows that the pool depletion, but not the rate of the vesicle pool depletion, is altered in Ca^{2+} dependent neurotransmitter release induced by 20 Hz stimulation in SNAP-25Δ9 – overexpressing neurons.

4.1.5 Recovery after high frequency stimulation with 20 Hz

I next determined the recovery of the vesicle pool after high frequency stimulation with 20 Hz by comparing the ratio between the amplitude of recovery EPSCs after high frequency stimulation and the amplitude of pretrain EPSCs. Therefore the mean and SEM of amplitude of the last 5 EPSCs of the 0.2 Hz stimulation before high frequency stimulation were used as the baseline and compared with the EPSC amplitude after high frequency stimulation for each cell. Data are presented in figure 4.1.7 .
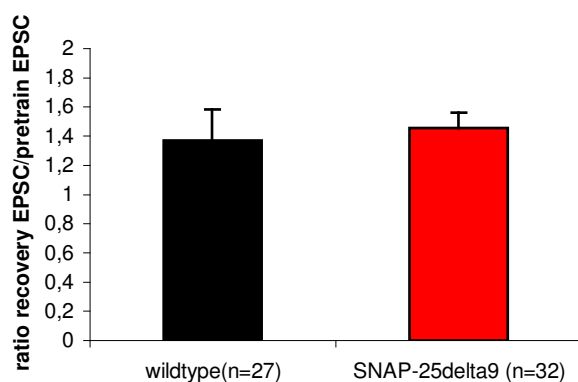
Figure 4.1.7: mean and SEM of the ratio of recovery EPSC to pretrain EPSC for 20 Hz stimulation: there was no significant difference between control group and SNAP-25Δ9 –overexpressing neurons (p= 0.107)

The mean ± SEM of the ratio of recovery EPSC to pretrain EPSC for wildtype neurons (n= 27) was 1.372 ± 0.212, for SNAP-25Δ9 – overexpressing neurons

(n= 32) 1.454 ± 0.108. There was no significant difference between these two groups, p= 0.107.

The ratio is greater than 1 due to the augmentation after high frequency stimulation, which induces a higher Ca^{2+} concentration in the cells and therefore more vesicles are staged for fusion and neurotransmitter release.

In order to investigate whether the recovery of the vesicle pools in case of high frequency stimulation and sucrose application are similar, I conferred the recoveries after 20 Hz stimulation, after first and after second sucrose application, as shown in figure 4.1.8 . The data of all cells – because there was no significant difference concerning the EPSC amplitudes between wildtype and SNAP-25Δ9– overexpressing neurons - were normalised to zero as starting point. My data demonstrate that there is a difference of replenishment after sucrose application and after high frequency stimulation as opposed to recent studies (Rosenmund and Stevens, 1996). The recovery after high frequency stimulation is quicker and achieves the final steady state earlier than after sucrose application.
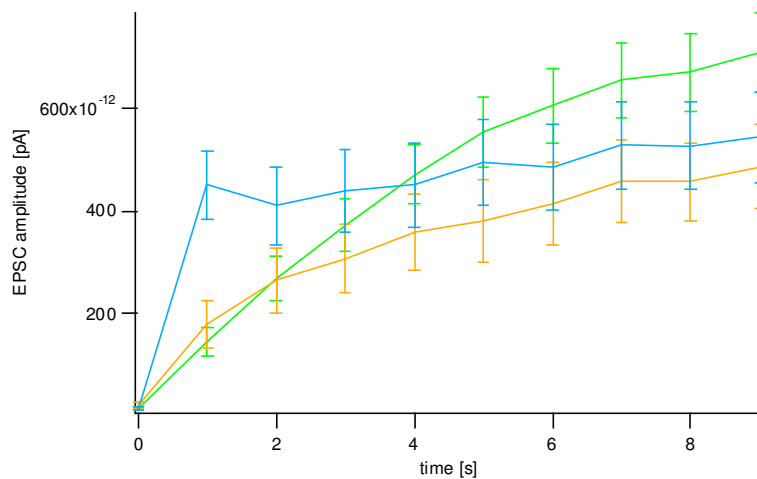
Figure 4.1.8: mean and SEM of normalised recovery after first sucrose application (green line, n= 74), after second sucrose application (orange line, n= 72) and after 20 Hz stimulation (blue line, n= 61) for wildtype and SNAP-25Δ9 – overexpressing neurons.

4.2   Deletion of SGT

To show the physiological role of SGT in hippocampal neurons in the molecular trimeric complex of CSP/SGT/Hsc70, I examined α/β-SGT double knockout mice. I wanted to prove whether there would be a similar physiological phenotype of α/β-SGT double knockout neurons than it was shown in case of CSPα lacking mice (Fernandez-Chacon et al., 2004).

All electrophysiological measurements on SGT neurons were performed in two stages to optimize pairing strategy of the double knockout mice: in the initial stage I compared wildtype neurons versus neurons from heterozygote mice. Since there was no statistical difference between these two cells groups, I compared in a second stage heterozygote versus double knockout neurons. In the following figures I show these two heterozygote groups as one control trace together.

4.2.1   Effect of SGT on postnatal day 8 - 14
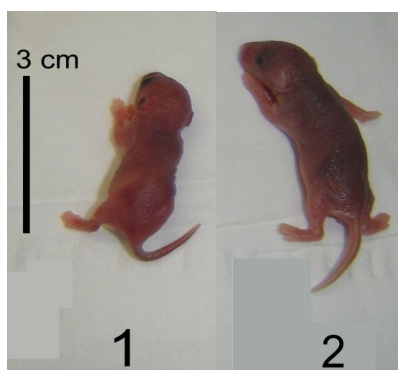
Figure 4.2.1.1: SGT littermate at P1 (1= double knockout mouse; 2= wildtype mouse).

Based on their phenotype, SGT double knockout mice could be distinguished at birth. The SGT double knockout mice at P0 were about 5 mm smaller than the other mice of the same litter. Besides small body size and low weight the SGT

double knockout mice were normal. They did not show obvious neurological or sensorimotor deficits during the first postnatal weeks.

The course of the electrophysiological measurements on SGT neurons is shown in figure 4.2.1.2. A 0.2 Hz stimulation period before and after each high frequency stimulation train serves as baseline for the experimental protocol and as guideline for the quality of the cell recording.
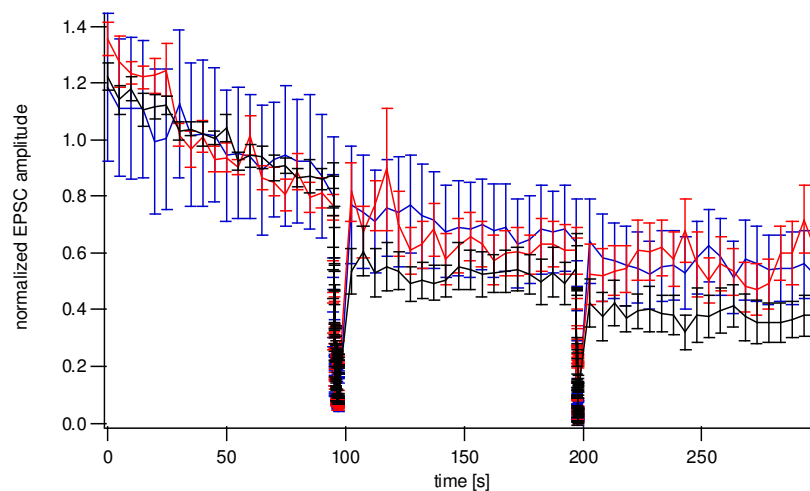
Figure 4.2.1.2:
normalised EPSC average and SEM of the cell-recordings during the whole protocol (0.2 Hz stimulation initially, 20 Hz stimulation, 0.2 Hz stimulation, 50 Hz stimulation and finally 0.2 Hz stimulation) for wildtype (n= 17; black), heterozygote (n= 32; blue) and knockout cells (n= 19; red) on P8-14. The 0.2 Hz stimulation between each high frequency stimulation train serves as baseline for the experimental protocol and as guideline for the quality of the cell recording.

4.2.1.1   Effect of SGT on EPSC amplitude on postnatal day 8 - 14

Initially I compared the EPSC amplitude, which was calculated from each cell during 0.2 Hz stimulation (20 stimuli), in hippocampal neurons of wildtype, heterozygote and SGT double knockout mice. The mean of EPSCs in wildtype cells was 1.19 ± 0.302 nA, n= 17, whereas EPSCs in heterozygote cells were 1.38 ± 0.153 nA, n= 32, and the mean of EPSCs in knockout cells was 1.21 ± 0.225 nA, n= 18. There was no significant difference in the EPSC amplitude of wildtype

compared to heterozygote neurons, p= 0.663, or wildtype and knockout neurons, p= 0.961, and heterozygote neurons compared to knockout neurons, p= 0.667. Data are presented in figure 4.2.1.3.
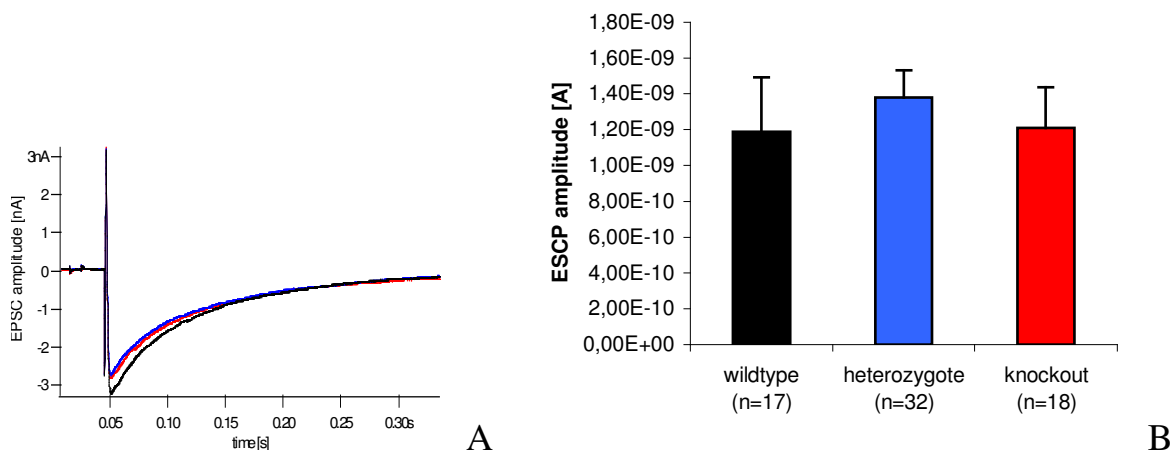
Figure 4.2.1.3:
A) exemplary traces of EPSC recording of wildtype (black), heterozygote (blue) and SGT-knockout neurons (red).
B) mean and SEM of EPSC amplitude of wildtype neurons (black, n= 17) was 1.19 ± 0.302 nA, of heterozygote cells (blue, n= 32) 1.38 ± 0.153 nA and of knockout neurons (red, n= 18) 1.21 ± 0.225 nA. Differences were insignificant between wildtype and heterozygote neurons, p= 0.663, wildtype and knockout neurons, p= 0.961, and heterozygote and knockout neurons, p= 0.667.

4.2.1.2 Effect on short-term depression induced by 20 Hz stimulation on postnatal day 8 - 14

In order to examine a potential effect of α/β-SGT on short-term synaptic plasticity, a stimulation protocol of 20 Hz (50 stimuli) for 2.5 s was carried out on wildtype, heterozygote and knockout neurons. The resulting EPSC amplitudes were normalised to the value of the last 4 responses of a 0.2 Hz stimulation, which served as the baseline during the entire experiment with these cells. The depression curves were plotted as a function of time.
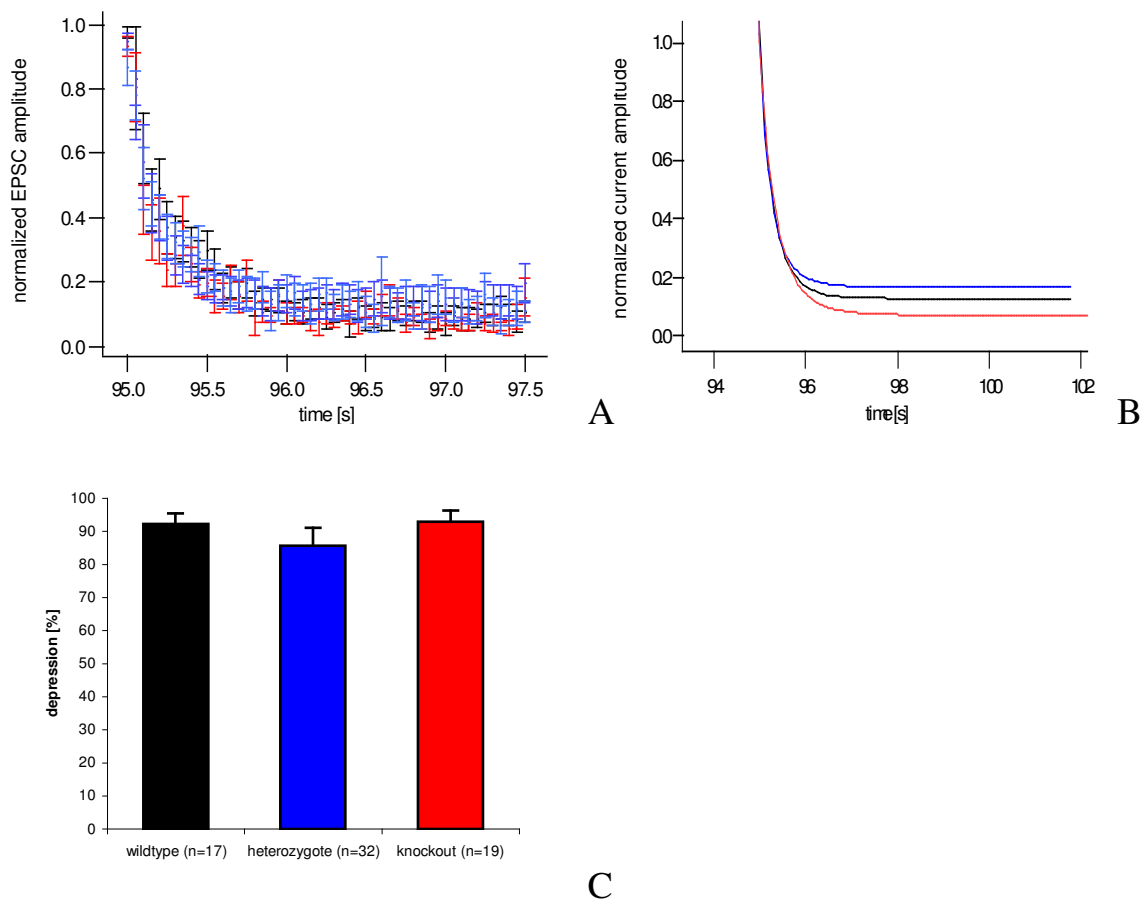
Figure 4.2.1.4:
A) mean and SEM of wildtype (black, n= 17), heterozygote (blue, n= 32) and knockout neurons (red, n= 19) during 20 Hz stimulation (50 stimuli). EPSC amplitudes normalised to the value of the last 4 responses of 0.2 Hz. The depression curves were plotted as a function of time.
B) average of fitted curves of wildtype neurons (black, n= 13), heterozygote (blue, n= 25) and knockout neurons (red, n= 17). All data of kinetics and pool depletion demonstrate no significant differences between the three control groups.
C) depression of wildtype (n= 17), heterozygote (n= 32) and knockout neurons (n= 19), p= 0.586 between wildtype and knockout and p= 0.689 between wildtype and heterozygote cells.

To obtain more detailed information about the kinetics of the pool depletion a double-exponential fit was applied to all data for 20 Hz trains as shown in the table 4.2.1.1:

	fast component (τ_{fast})	slow component (τ_{slow})	steady state (y_0)
wildtype neurons (n= 13)	0.182 $\pm$ 0.069 s	0.394 $\pm$ 0.067 s	0.077 $\pm$ 0.032 s
heterozygote neurons (n= 25)	0.191 $\pm$ 0.030 s	0.452 $\pm$ 0.109 s	0.143 $\pm$ 0.054 s
knockout neurons (n= 17)	0.285 $\pm$ 0.163 s	0.534 $\pm$ 0.053 s	0.071 $\pm$ 0.034 s

Table 4.2.1.1: summary of the fitted data of 20 Hz stimulation (values are given as mean $\pm$ SEM [s])

There was no significant difference in the rate of pool depletion of these three groups (data see table 4.2.1.1), p= 0.676 between wildtype and knockout, p= 0.442 between wildtype and heterozygote and p= 0.238 between heterozygote and knockout neurons for the rapid decay component τ_{fast}. The analysis of τ_{slow} resulted in p= 0.109 for wildtype and knockout cells, p= 0.365 for wildtype and heterozygote and p= 0.110 for heterozygote and knockout neurons. The degree of depression achieved at 20 Hz stimulation, steady state y_0, was not significantly different for SGT - knockout neurons compared to wildtype cells, p= 0.586. The steady state y_0 was not significantly different for heterozygote neurons, p= 0.689, as compared to wildtype cells, and p= 0.682, compared to knockout cells.

These results demonstrate that neither rates of pool depletion nor the degree of depletion of vesicle pools is changed in neurons of SGT - mutants during high frequency stimulation at 20 Hz.

4.2.1.3 Effect on short-term depression induced by 50 Hz stimulation on postnatal day 8 - 14

To determine whether there are changes in short term depression following stimulation with higher frequency, a protocol of 50 Hz (30 stimuli) for 0.6 s was carried out on wildtype, heterozygote and knockout neurons. The resulting EPSC amplitudes were normalised to the value of the last 4 responses obtained at 0.2 Hz stimulation serving as the baseline for the analysis of the high frequency stimulation protocol. The depression curves were plotted as a function of time.
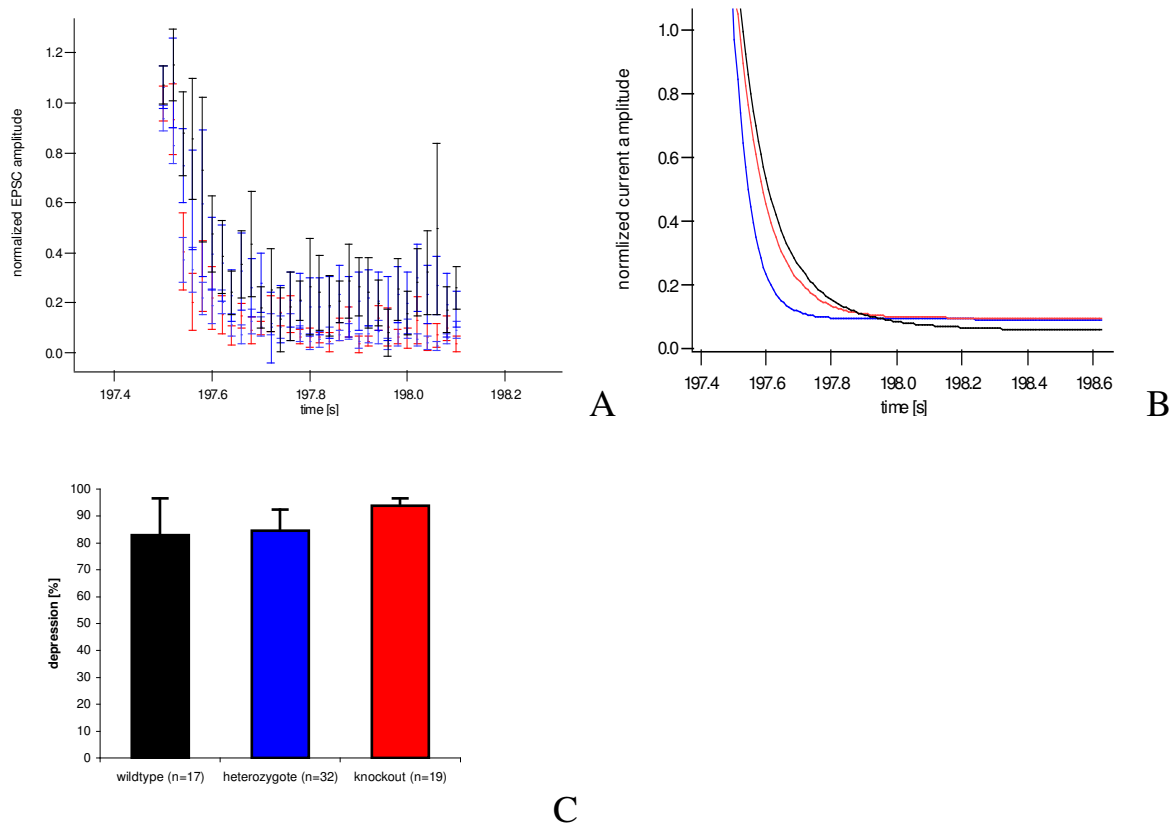
Figure 4.2.1.5:
A) average and SEM of wildtype (black, n= 17), heterozygote (blue, n= 32) and knockout neurons (red, n= 19) during 50 Hz stimulation (30 stimuli). EPSC amplitudes normalised to the value of the last 4 responses of 0.2 Hz. The depression curves were plotted as a function of time.
B) average of fitted curves; wildtype neurons (black, n= 13), heterozygote (blue, n= 25) and knockout neurons (red, n= 17). All data of kinetics and pool depletion demonstrate no significant differences between the three control groups.
C) depression of wildtype (n= 14), heterozygote (n= 26) and knockout neurons (n= 15), p= 0.836 between wildtype and knockout and p= 0.756 between wildtype and heterozygote cells.

To determine the rate of depression, a double-exponential fit was applied to these curves. The results are shown in the table 4.2.1.2:

	fast component (τ_{fast})	slow component (τ_{slow})	steady state (y_0)
wildtype neurons (n= 14)	0.087 ± 0.013 s	0.200 ± 0.078 s	0.170 ± 0.137 s
heterozygote neurons (n= 26)	0.070 ± 0.016 s	0.297 ± 0.085 s	0.155 ± 0.080 s
knockout neurons (n= 15)	0.086 ± 0.031s	0.096 ± 0.046 s	0.061 ± 0.028 s

Table 4.2.1.2: summary of the fitted data of 50Hz stimulation (values are given as mean ± SEM [s])

The data were well fit with a double-exponential decay. There was no significant change in rate of pool depletion during high frequency stimulation with 50 Hz in one of these three groups (data shown in table 4.2.1.2), p= 0.132 between wildtype and knockout, p= 0.086 between wildtype and heterozygote and p= 0.860 between heterozygote and knockout neurons for the rapid decay time constant τ_{fast}. Neither there was any significant difference between these three groups for the slow decay time constant τ_{slow}: p= 0.184 for wildtype and knockout cells, p= 0.655 for wildtype and heterozygote and p= 0.102 for heterozygote and knockout neurons. The degree of depression, the steady state y_0, was not significantly different for SGT - knockout neurons as compared to wildtype cells, p= 0.836. And the steady state y_0 was also not significantly different for heterozygote neurons, p= 0.756, compared to wildtype cells, and p= 0.839, when compared to knockout cells.

These results demonstrate that the short term depression is faster during higher frequency stimulation trains, as expected (Zucker and Regehr, 2002; Taschenberger et al., 2005). However neither the kinetic rates of pool depletion nor

the degree of pool depletion is changed in SGT - mutants during high frequency stimulation of 50 Hz.

4.2.1.4 Effect of SGT on vesicle pool

In order to test whether the pool size of SGT double knockout neurons is altered, the pool size was determined by 5 s lasting application of hypertonic sucrose solution, which leads to a Ca^{2+} independent release of all releasable vesicles. Exemplary Traces of synaptic responses of application of hypertonic sucrose solution are shown in figure 4.2.1.6. The integral of charge transfer during hypertonic sucrose application was used as an estimation of the total pool size.
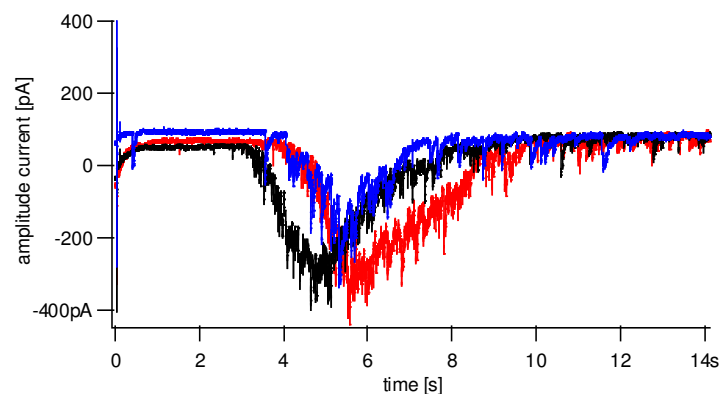
Figure 4.2.1.6:
exemplary normalised traces of application of hypertonic sucrose solution for wildtype (black), heterozygote (blue) and knockout neurons (red).

As seen in the case of synaptically evoked responses (figure 4.2.1.3), excitatory responses induced by application of hypertonic sucrose solution were not reduced neither in SGT double knockout nor in heterozygote mice (figure 4.2.1.7). The mean of total charge transfer during the sucrose application after 0.2 Hz stimulation was 0.87 ± 0.496 nC, n= 11, for control cells, 0.574 ± 0.207 nC, n= 6, for heterozygote neurons and 0.965 ± 0.799 nC, n= 7, for knockout neurons. The results indicate no differences in pool size between SGT - heterozygote and

knockout neurons, p= 0.295, and between wildtype and knockout neurons, p= 0.526, or between wildtype and heterozygote neurons, p= 0.651.
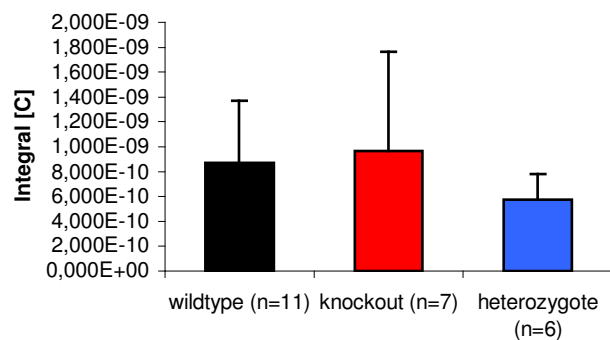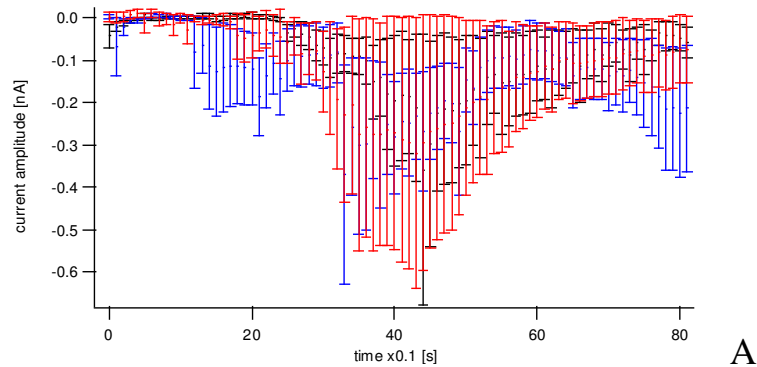
Figure 4.2.1.7:
A) average and SEM of sucrose application from wildtype (n= 11; black), heterozygote neurons (n= 6; blue) and knockout neurons (n= 7; red). Data are normalised to a baseline of 0 nA.
B) mean of total current transfer during the sucrose application after 0.2 Hz stimulation was noted as 0.87 ± 0.496 nC, n= 11, for control cells, 0.574 ± 0.207 nC, n= 6, for heterozygote and 0.965 ± 0.799 nC, n= 7, for knockout neurons. The results indicate no differences of the pool size between SGT - heterozygote and knockout neurons, p= 0.295, and between wildtype and knockout neurons, p= 0.526, or between wildtype and heterozygote neurons, p= 0.651.

4.2.2   Effect of SGT on postnatal day 21 - 24

At P21 the knockout mice were about 15 mm smaller than the other mice of the same litter. Besides the smaller body size and lower weight the phenotype of the SGT double knockout mice was inconspicuous. They did not show any obvious neurological or sensorimotor deficits during the first postnatal weeks until P28 as observed in CSPα knockout mice (Fernandez-Chacon et al., 2004). There was no increase of mortality of SGT double knockout in the first postnatal months.

With electrophysiological measurements in approximately three week old hippocampal neurons in culture, I wanted to determine if SGT double knockout mice show additional deficits. Cause of the idea of a function as cochaperone of SGT protein of the trimeric complex of CSP/SGT/Hsc70 the loss of SGT could lead to no severe changes of the extrinsic phenotype but to changes of the EPSC amplitudes and short-term depression.

Generally, recording EPSCs from neurons in culture at day P21 until P24 was more difficult because of the large size of these older neurons and the huge dendritic trees increasing in three weeks old cell cultures. It was also very difficult to maintain neurons longer than three weeks in cell culture. So the number of experiments on neurons at P21 to P24 is low and the SEM higher than in the previous results from SGT neurons on P8-14. Since I did not see a significant effect of the phenotype and EPSC recordings of SGT knockout mice after previous experiments, I did not perform further experiments because I did not expect a significant effect of SGT concerning the synaptic function or neurotransmitter release in these mice.
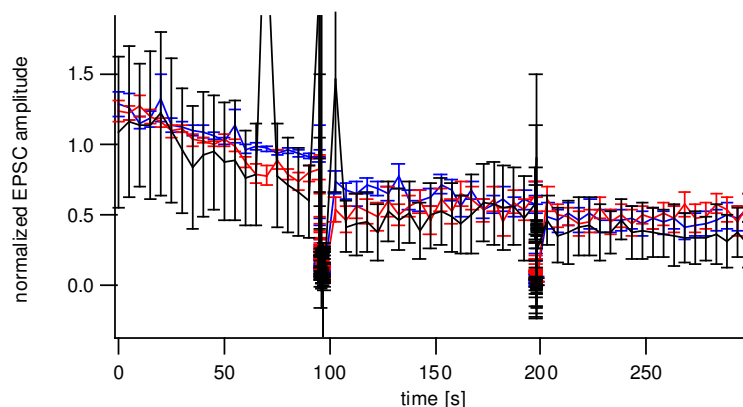
Figure 4.2.2.1:

Normalised EPSC average and SEM of the cell-recordings during the whole protocol (0.2 Hz stimulation initially, 20 Hz stimulation, 0.2 Hz stimulation, 50 Hz stimulation and finally 0.2 Hz stimulation) for wildtype (n= 9, black), heterozygote (n= 11, blue) and knockout cells (n= 5, red) on P21-24.

4.2.2.1   Effect of SGT on EPSC amplitude on postnatal day 21 - 24

Initially the mean of EPSC amplitude was calculated as the mean of each cell during 0.2 Hz stimulation (20 stimuli). The mean amplitude of wildtype cells was 2.68 ± 1.09 nA, n= 5, of heterozygote cells 3.01 ± 0.624 nA, n= 11, and of knockout cells 2.90 ± 0.659 nA, n= 9. There was no significant difference concerning the EPSC amplitude of wildtype and heterozygote neurons, p= 0.783, wildtype and knockout neurons, p= 0.854, and heterozygote and knockout neurons, p= 0.908. These results indicate no change in EPSCs in SGT lacking mice on P21-24.
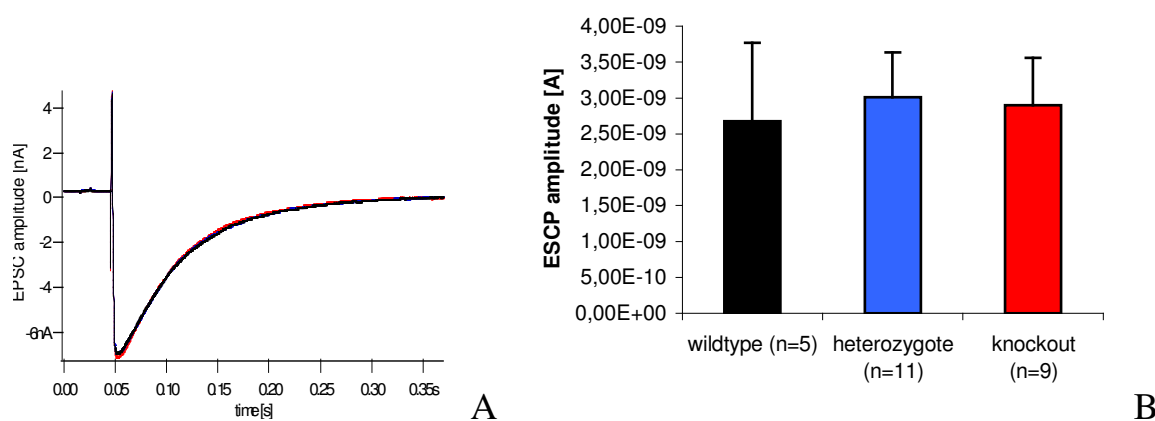
Figure 4.2.2.2:
A) exemplary traces of EPSC recording P21-24.
B) EPSC amplitude of wildtype (black, n= 5), heterozygote (blue, n= 11) and knockout hippocampal neurons (red, n= 9) on P21-24. The mean of wildtype cells was 2.68 ± 1.09 nA, n= 5, of heterozygote cells 3.01 ±0.624 nA, n= 11, and of knockout cells 2.90 ±0.659 nA, n= 9. There was no significant difference between wildtype and heterozygote neurons, p= 0.783, wildtype and knockout neurons, p= 0.854, and heterozygote and knockout neurons, p= 0.908.

4.2.2.2 Effect on short-term depression induced by 20 Hz stimulation on postnatal day 21 - 24

I used the same high frequency stimulation protocol as on P8-14 to examine synaptic currents in neurons at P21-24. Neurons of each group were stimulated with 20 Hz (50 stimuli) for 2.5 s. The resulting EPSC amplitudes were normalised to the value of the last 4 responses of 0.2 Hz serving as the baseline for the analysis of the high frequency stimulation protocol. The depression curves were plotted as function of time.
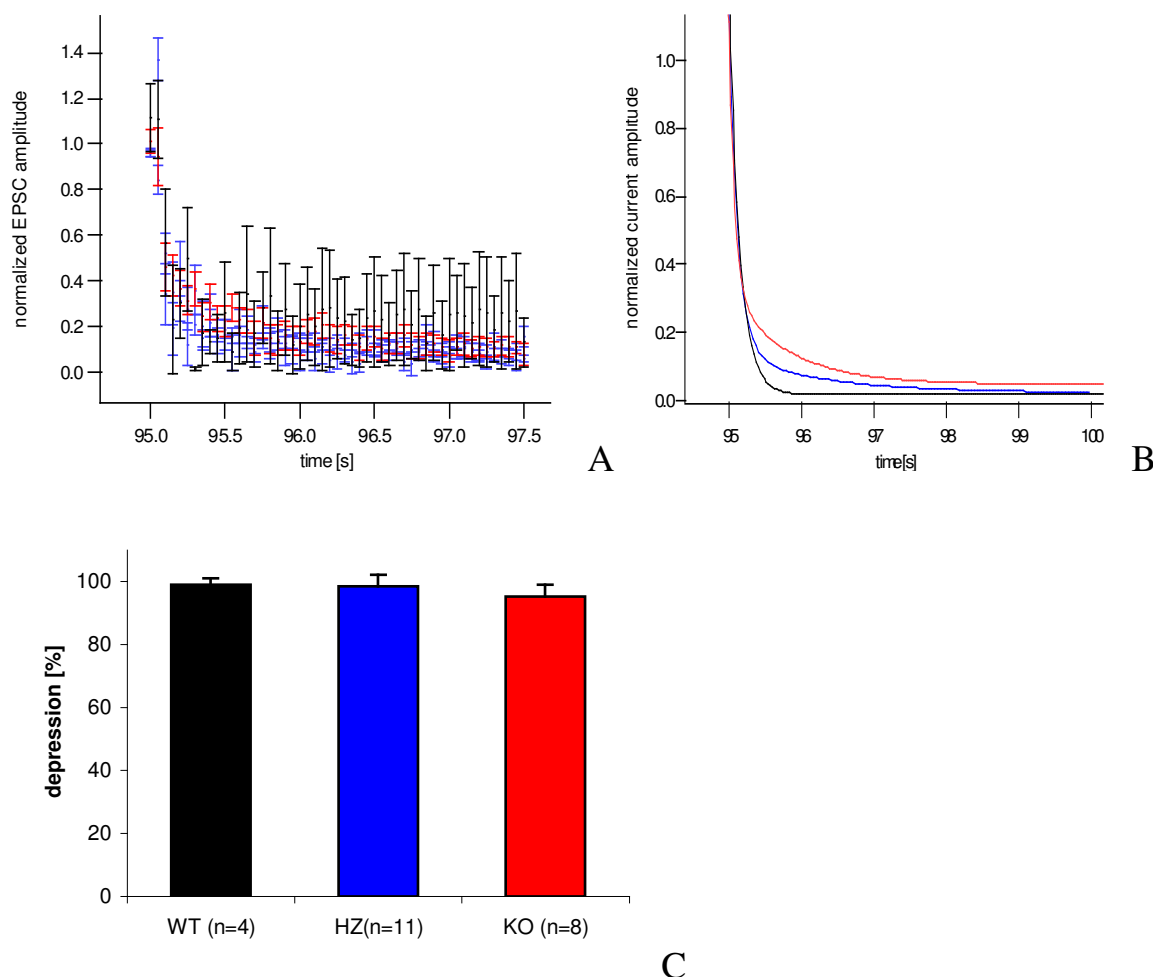
Figure 4.2.2.3:
A) average and SEM of wildtype (black, n= 5), heterozygote (blue, n= 11) and knockout neurons (red, n= 9) during 20 Hz stimulation (50 stimuli). EPSC amplitudes normalised to the value of the last 4 responses of 0.2 Hz. The depression curves were plotted as a function of time.

B) average of fitted curves. Wildtype neurons (black, n= 4), heterozygote (blue, n= 11) and knockout neurons (red, n= 8). τ_{fast} and steady state y_0 was nonsignificant for all control groups. τ_{slow} was significantly reduced between these three groups, p= 0.012 for wildtype and knockout cells, p= 0.192 for wildtype and heterozygote and p= 0.967 for heterozygote and knockout neurons.
C) depression of wildtype (n= 4), heterozygote (n= 11) and knockout neurons (n= 8), p= 0.710 between wildtype and knockout and p= 0.994 between wildtype and heterozygote cells.

The rate of the pool depletion was determined using a double-exponential fit as shown in the table 4.2.2.1:

	fast component (τ_{fast})	slow component (τ_{slow})	steady state (y_0)
wildtype neurons (n= 4)	0.152 ± 0.052 s	0.138 ± 0.058 s	0.010 ± 0.021 s
heterozygote neurons (n= 11)	0.122 ± 0.025 s	0.766 ± 0.341 s	0.016 ± 0.038 s
knockout neurons (n= 8)	0.082 ± 0.023 s	0.773 ± 0.089 s	0.048 ± 0.038 s

Table 4.2.2.1: summary of the fitted data of 20 Hz stimulation on P21-24 (values are given as mean $\pm$ SEM [s])

Pool depletion during high frequency stimulation with 20 Hz depends on a fast decay τ_{fast}, which was neither significantly different for wildtype and knockout, p= 0.118, nor for wildtype and heterozygote p= 0.597, nor for heterozygote and knockout neurons, p= 0.139 (data shown in table 4.2.2.1).

But there was a significant difference between these three groups for the time constant τ_{slow}, p= 0.012 for wildtype and knockout cells, p= 0.192 for wildtype and heterozygote and p= 0.967 for heterozygote and knockout neurons.

The degree of depression, the steady state y_0, was not significantly different for SGT - knockout neurons compared to wildtype cells, p= 0.710. Neither the steady

state y_0 was not different for heterozygote neurons, p= 0.994, compared to wildtype cells, or p= 0.664, compared to knockout cells.

These results demonstrate that, with the exception of a minor reduction of the slow component of depression, there are no differences in excitatory synaptic transmission in SGT double knockout mice. There were no differences in the phenotype on P21-24, so that we did not attribute great importance to the reduction of the slow component of depression – also cause of the small number of experiments with three weeks old neurons.

4.2.2.3   Effect on short-term depression induced by 50 Hz stimulation on postnatal day 21 - 24

As in case of the 50 Hz stimulation on P8-14, the neurons at P21-24 of each group were stimulated with 50 Hz (30 stimuli) for 0.6 s. The resulting EPSC amplitudes were normalised to the value of the last 4 responses of 0.2 Hz and served as a the baseline during the entire experiments on these cells. The depression curves were plotted as a function of time.
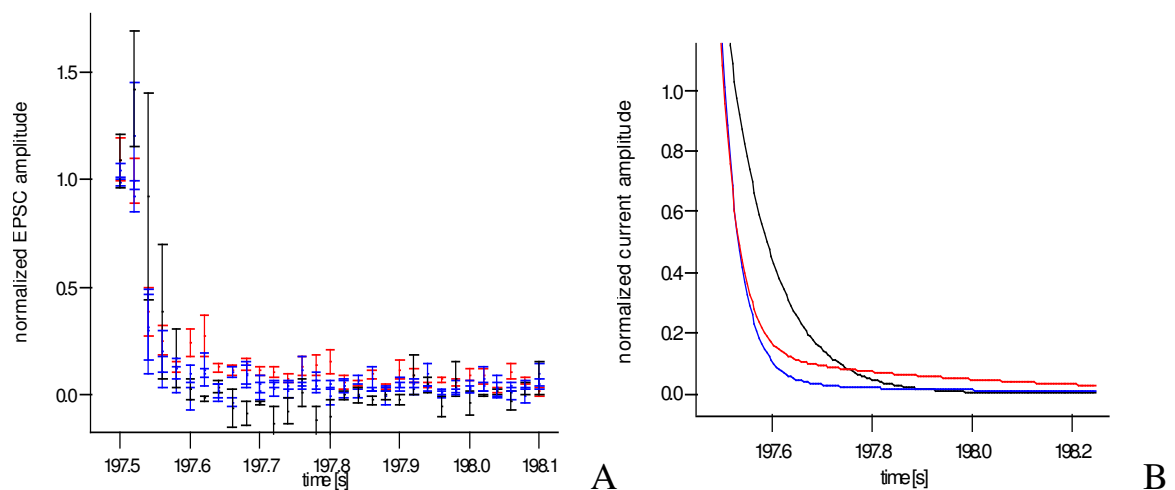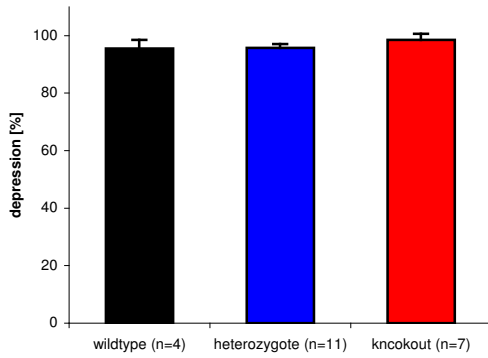
C

Figure 4.2.2.4:
A) average and SEM of wildtype (black, n= 5), heterozygote (blue, n= 11) and knockout neurons (red, n= 9) during 50 Hz stimulation (30 stimuli). EPSC amplitudes were normalised to the value of the last 4 responses of 0.2 Hz, which served as the baseline during all experiments on these cells. The depression curves were plotted as a function of time.
B) average of fitted curves. Wildtype neurons (black, n= 4), heterozygote (blue, n= 11) and knockout neurons (red, n= 7). τ_{fast} and steady state y_0 was nonsignificant for all control groups. τ_{slow} was significantly reduced between these three groups, p= 0.002 for wildtype and knockout cells, p= 0.473 for wildtype and heterozygote and p= 0.043 for heterozygote and knockout neurons.
C) depression of wildtype (n= 4), heterozygote (n= 11) and knockout neurons (n= 7), p= 0.683 between wildtype and knockout and p= 0.215 between wildtype and heterozygote cells.

The depression curves were fitted with a double-exponential fit. The results are shown in table 4.2.2.2:

	fast component (τ_{fast})	slow component (τ_{slow})	steady state (y_0)
wildtype neurons (n= 4)	0.091 ± 0.013 s	0.081 ± 0.020 s	0.045 ± 0.030 s
heterozygote neurons (n= 11)	0.037 ± 0.014 s	0.369 ± 0.171 s	0.042 ± 0.013 s
knockout neurons (n= 7)	0.036 ± 0.004 s	0.565 ± 0.095 s	0.015 ± 0.022 s

Table 4.2.2.2: summary of the fitted data of 50 Hz stimulation on P21-24 (values are given as mean ± SEM [s])

Pool depletion during high frequency stimulation with 50 Hz showed no significant difference for the fast decay τ_{fast}, p= 0.283 between wildtype and knockout, p= 0.170 between wildtype and heterozygote and p= 0.433 between heterozygote and knockout neurons (data see table 4.2.2.2).

The differences between these three groups for the slow time constant τ_{slow} were significant, p= 0.002 for wildtype and knockout cells, p= 0.473 for wildtype and heterozygote and p= 0.043 for heterozygote and knockout neurons.

The degree of depression, the steady state y_0, was not significantly different for SGT double knockout neurons as compared to wildtype cells, p= 0.683, nor was the steady state y_0 significantly different for heterozygote neurons as compared to wildtype cells, p= 0.215, or p= 0.181, as compared to knockout cells, too.

These results demonstrate that there is a minor reduction of the slow component in knockout neurons comparable to 20 Hz stimulation on P21-24 and that the short-term depression occurs more rapidly during higher frequency stimulation trains as shown in case of the data obtained from P8-14. All other results offer no significant difference between the three control groups.

5. Discussion

5.1 SNAP-25

5.1.1 Overexpression of SNAP-25Δ9 reduces the release probability and has the same effect as cleavage with BoNT/A in neurons

In the current study I have compared the effect of native SNAP-25 and of overexpressed Δ9 - mutant of SNAP-25 on neurotransmitter release in hippocampal neurons.

Overexpression of SNAP-25Δ9, in which the last nine C-terminal amino acids are lacking, led to a reduction of the release probability and thereby to a reduction of synaptic depression at excitatory synapses. SNAP-25Δ9 - overexpressing neurons also had a reduced releasable pool size, but there was no effect on the rates of release of the vesicle pools during short-term depression induced by high frequency stimulation at physiological Ca^{2+} concentrations. Higher extracellular calcium concentrations can partly overcome this reduction of the releasable pool size as shown in recent reports on chromaffin cells (Sorensen et al., 2006).

Previous data on chromaffin cells overexpressing SNAP-25Δ9 showed a selective reduction of the fast component and were interpreted as a selective loss of the RRP, while the SRP persisted (Wei et al., 2000). This and my findings are in agreement with data obtained in neurons after BoNT/A treatment (Trudeau et al., 1998; Gerona et al., 2000; Sakaba et al., 2005) and previous studies using BoNT/A to cleave endogenous SNAP-25 (Xu et al., 1998), which demonstrated a partially suppression of exocytosis in neurons manifested at the fast and the slow component by retarding the reactions in which SNAP-25 is involved. Thereby BoNT/A strongly reduced the apparent Ca^{2+} sensitivity.

SNAP-25Δ9 - overexpressing neurons exhibit a dual exponential decay of EPSC size during high frequency stimulations. The presence of two components of

depression is likely due to existence of two different vesicle pools, the SRP and the RRP.

In recent studies of BoNT in chromaffin cells, it was postulated that treatment with BoNT alters the kinetics of release. These studies drew conclusions based on the fusion of many vesicles over a time course of seconds to tens of minutes. Under these conditions it is difficult to observe directly whether release of individual vesicles is impaired by a reduction in the probability of vesicle fusion or by a slowing of release kinetics, or by both (Poulain et al., 1996; Criado et al., 1999). My results indicate, that the rate of release is not modified in neurons; rather, the release probability of single synaptic vesicles is altered resulting in a reduction of the RRP.

5.1.2 The RRP is not altered in SNAP-25Δ9 - overexpressing neurons as determined by hypertonic sucrose application

The total charge released during application of hypertonic sucrose by SNAP-25Δ9 - overexpressing neurons was similar to that released by wildtype neurons. This result is consistent with recent studies, that demonstrate a Ca^{2+} independent mechanism of neurotransmitter release for application of hypertonic solution (Rosenmund and Stevens, 1996). The slight reduction of response in case of sucrose application after high frequency stimulation corresponds to the short term depression of EPSCs after high frequency stimulation as reported in previous proceedings in case of sucrose application (Rosenmund and Stevens, 1996).

The recovery of synaptic transmission in the SNAP-25Δ9 - overexpressing neurons is not significantly altered after sucrose induced release or after high frequency stimulation. But recovery after sucrose application takes more time and achieves the final steady state later than in case of high frequency stimulation. This fact suggests that pool recovery was not complete at the start of high frequency stimulation with 20 Hz after a prior sucrose solution stimulation (see figure 4.1.6 A). Therefore I should wait longer between the different stimulation protocols for

achieving a complete replenishment of the vesicle pools after each stimulation. Also, in recent studies it was reported that after the readily releasable pool has been depleted, it recovers with a time constant near 8 s (Stevens and Tsujimoto, 1995). Thus, in future experiments I will wait longer after stimuli to achieve a complete replenishment.

My results demonstrate that the postulated RRP in neurons (Rosenmund and Stevens, 1996) is not comparable with the RRP in chromaffin cells (as reported by Rettig and Neher, 2002), because the RRP is eliminated in SNAP-25Δ9 - overexpressing chromaffin cells and after treatment with BoNT/A, while it persisted in my experiments on hippocampal neurons. Similar results were shown in synaptotagmin 1 lacking mice (Geppert et al., 1994): which have normal neurotransmitter release after hypertonic sucrose application, whereas Ca^{2+} mediated release is severely attenuated in these animals.

The most likely release mechanism induced by hypertonic sucrose is a mechanical one like a stress induced change caused by the hypertonic treatment (Zenchenko and Morozov, 1995), which delivers the sufficient energy for the release of all primed vesicles. Application of hypertonic solution produces a visible decrease in the volume of neuron cell bodies, of the neuronal dendrites and of the axons in the region of application. Deformation may supply additional energy, overcoming the energy barrier for fusion, which is normally very high.

The identity of the vesicle pools, which are depleted by treatment with hypertonic sucrose solutions, is not clear. My data indicate that not only the RRP is released by sucrose application, as reported in recent studies, but that the SRP and UPP are also released. The charge transfer in the SNAP-25Δ9 - mutants is not reduced following hypertonic solution treatment. In addition responses during sucrose application would be smaller or would be delayed, if release occurred only in vesicles of the SRP because the SRP cannot refill both, the RRP and SRP itself in a few seconds. Third, recovery after sucrose application takes longer and the degree of recovery is lower than that observed after high frequency stimulation. This is contrary to previous results (Rosenmund and Stevens, 1996), in which recovery was shown to reach the steady state more quickly, suggesting, that not only the RRP and SRP were released as in case of high frequency stimulation but also the

UPP was released, which requires a longer replenishment period. If the same releasable pools of vesicles were released by these two release mechanisms, recovery should have a similar time course.

The release mechanism induced by hypertonic sucrose is Ca^{2+} independent and doesn't need primed vesicles for release. Thereby this mechanism of shrinking, which is induced by sucrose application, delivers the energy, which is needed for release of all docked vesicles, which are staying at the plasma membrane directly: RRP, SRP and UPP. The release, which is produced by hypertonic sucrose solution, would engage the exocytotic machinery at some step after docking.

5.1.3 EPSC amplitude is not altered in SNAP-25Δ9 - overexpressing neurons

The EPSC amplitude of SNAP-25Δ9 - overexpressing neurons is not reduced in comparison to wildtype neurons. This is unexpected, since one would expect a reduced EPSC amplitude caused by the reduction in release probability.

It is possible that the reduction of release probability is not apparent at the beginning of low frequency stimulation and appears only after a longer period of stronger stimulation.

Another possible explanation is the so-called ´synaptic scaling`. Synaptic scaling is a bidirectional phenomenon in which excitatory synapses scale up in response to activity reduction and scale down in response to increases in activity (Trudeau et al., 1998; Turrigiano and Nelson, 2004; Pawlak et al., 2005). Synaptic scaling serves to maintain the strengths of synapses relative to each other, lowering amplitudes of small EPSCs in response to continual excitation and raising them after prolonged blockage or inhibition (Perez-Otano and Ehlers, 2005). In my results, the reduced release probability could be matched by synaptic scaling and therefore masking the effects on EPSC amplitude in the SNAP-25Δ9 - mutants.

Finally, reduction in EPSC amplitude was reported upon BoNT/A treatment (Xu et al., 1998). My experimental approach with overexpression of SNAP-25Δ9 is

different, although both approaches yield the same protein. Overexpression of proteins uses an endogenous biomolecular pathway and infection of proteins an exogenous pathway. Thus, I cannot compare my results with those reported upon BoNT/A treatment directly.

5.2   Effect of SGT on synaptic transmission

5.2.1 Effect of SGT on postnatal day 8 - 14

The SGT lacking mice do not exhibit any obvious deficits or changes in EPSC amplitude or kinetics at P8-14. Neither the action potential dependent release nor the vesicle pool sizes are altered. Thus, the loss of the α- and β-SGT protein does not appear to alter the physiological function or maintenance of the neuronal synapses during this time period.

Since the synaptic function in SGT double knockout mice was unaltered and because of the reported development of synaptic function in CSPα lacking mice (Fernandez-Chacon et al., 2004), I decided to measure the electrophysiological synaptic function in neurons of mice that are older than three weeks.

5.2.2 Effect of SGT on postnatal day 21 - 24

The SGT double knockout mice recorded on P21-24 do not exhibit reduced EPSC amplitude, changes of kinetics or a change in releasable pool size.

Unfortunately, the number of experiments, I have completed with neurons from those mice, is limited. It has been very difficult to record from neurons after more than three weeks in cell culture, so it was only possible to measure few cells. I decided not to do additional experiments, because the preliminary experiments and analysis were not promising. It is quite unlikely that additional experiments would

have led to a significant difference between wild type and SGT double knockout neurons.

It appears that the α- and β-SGT protein has no effect on neurotransmitter release in these cells.

5.2.3 Physiological role of SGT-protein in neurons

The latest reports allude to the function of SGT as a cochaperone in complexes with the Hsc protein family and the Hsp protein family in cell division (Winnefeld et al., 2004; Liou and Wang, 2005; Winnefeld et al., 2006; Yin et al., 2006) and to an important role of SGT in apoptotic signalling (Wang et al., 2005). Recent studies on α-SGT and the brain specific isoform β-SGT report an inhibition of neurotransmitter release in SGT overexpressing neurons in culture, suggesting that the CSP/SGT/Hsc70 complex is important for the maintenance of a normal synaptic function (Tobaben et al., 2001). My results do not support an important role of SGT in synaptic transmission of neurons. Neurons cultured at P0 and maintained in culture for 10 to 24 days exhibited normal EPSC amplitude, normal short-term plasticity and unaltered pool size.

SGT is part of the synaptic trimeric complex CSP/SGT/Hsc70 in neurons as reported in recent studies and it probably acts as cochaperone of CSP (Tobaben et al., 2001; Tobaben et al., 2003). CSP is the most important part of this chaperone complex – because of the obvious severe dysfunction of the synapse on the presynapse in CSPα lacking mice (Fernandez-Chacon et al., 2004). SGT and Hsc70 act as cochaperones. The loss of SGT does not result in severe functional deficits or death of the knockout mice. There may be an effect in older mice, but I did not observe any effects in SGT lacking mice in the timeframe of about 3 to 4 weeks in my measurements except of the body size of these mice.

The synaptic transmission is not strongly affected by the loss of SGT. I cannot exclude the possibility of a compensation by Hsc70, which allows normal function

of the presynaptic machinery in absence of SGT. But my results challenge the role of SGT as an important cochaperone in neurons.

5.2.4 Outlook

It will be interesting to determine whether Hsc70 lacking mice would present a similar phenotype and electrophysiological responses as SGT double knockout mice. Hsc70 lacking mice may exhibit a dysfunction of the synaptic transmission similar to that, which was observed in CSPα lacking mice. This would indicate a more important function of Hsc70 than of SGT as cochaperone of CSP.

As a follow up, if Hsc70 knockout mice were shown to exhibit similar effects as SGT knockout mice, would be measurements on α-/β-SGT/Hsc70 knockout mice to investigate the physiological role and importance of both cochaperones for the presynaptic proteins together. It may be that the function of the presynaptic chaperone complex is maintained only with the most important protein CSP.

6. References

1. Angeletti PC, Walker D, Panganiban AT (2002) Small glutamine-rich protein/viral protein U-binding protein is a novel cochaperone that affects heat shock protein 70 activity. Cell Stress Chaperones 7:258-268.

2. Aravamudan B, Fergestad T, Davis WS, Rodesch CK, Broadie K (1999) Drosophila UNC-13 is essential for synaptic transmission. Nat Neurosci 2:965-971.

3. Ashery U, Betz A, Xu T, Brose N, Rettig J (1999) An efficient method for infection of adrenal chromaffin cells using the Semliki Forest virus gene expression system. Eur J Cell Biol 78:525-532.

4. Ashery U, Varoqueaux F, Voets T, Betz A, Thakur P, Koch H, Neher E, Brose N, Rettig J (2000) Munc13-1 acts as a priming factor for large dense-core vesicles in bovine chromaffin cells. Embo J 19:3586-3596.

5. Augustin I, Rosenmund C, Sudhof TC, Brose N (1999) Munc13-1 is essential for fusion competence of glutamatergic synaptic vesicles. Nature 400:457-461.

6. Bark IC, Hahn KM, Ryabinin AE, Wilson MC (1995) Differential expression of SNAP-25 protein isoforms during divergent vesicle fusion events of neural development. Proc Natl Acad Sci U S A 92:1510-1514.

7. Bekkers JM, Stevens CF (1991) Excitatory and inhibitory autaptic currents in isolated hippocampal neurons maintained in cell culture. Proc Natl Acad Sci U S A 88:7834-7838.

8. Betz WJ (1970) Depression of transmitter release at the neuromuscular junction of the frog. J Physiol 206:629-644.

9. Blioch ZL, Glagoleva IM, Liberman EA, Nenashev VA (1968) A study of the mechanism of quantal transmitter release at a chemical synapse. J Physiol 199:11-35.

10. Bock JB, Matern HT, Peden AA, Scheller RH (2001) A genomic perspective on membrane compartment organization. Nature 409:839-841.

11. Borisovska M, Zhao Y, Tsytsyura Y, Glyvuk N, Takamori S, Matti U, Rettig J, Sudhof T, Bruns D (2005) v-SNAREs control exocytosis of vesicles from priming to fusion. Embo J 24:2114-2126.

12. Brose N, Rosenmund C, Rettig J (2000) Regulation of transmitter release by Unc-13 and its homologues. Curr Opin Neurobiol 10:303-311.

13. Callahan MA, Handley MA, Lee YH, Talbot KJ, Harper JW, Panganiban AT (1998) Functional interaction of human immunodeficiency virus type 1 Vpu and Gag with a novel member of the tetratricopeptide repeat protein family. J Virol 72:8461.

14. Capogna M, McKinney RA, O'Connor V, Gahwiler BH, Thompson SM (1997) Ca2+ or Sr2+ partially rescues synaptic transmission in hippocampal cultures treated with botulinum toxin A and C, but not tetanus toxin. J Neurosci 17:7190-7202.

15. Chapman ER, An S, Barton N, Jahn R (1994) SNAP-25, a t-SNARE which binds to both syntaxin and synaptobrevin via domains that may form coiled coils. J Biol Chem 269:27427-27432.

16. Chen YA, Scheller RH (2001) SNARE-mediated membrane fusion. Nat Rev Mol Cell Biol 2:98-106.

17. Criado M, Gil A, Viniegra S, Gutierrez LM (1999) A single amino acid near the C terminus of the synaptosomeassociated protein of 25 kDa (SNAP-25) is essential for exocytosis in chromaffin cells. Proc Natl Acad Sci U S A 96:7256-7261.

18. Cziepluch C, Kordes E, Poirey R, Grewenig A, Rommelaere J, Jauniaux JC (1998) Identification of a novel cellular TPR-containing protein, SGT, that interacts with the nonstructural protein NS1 of parvovirus H-1. J Virol 72:4149-4156.

19. Elmqvist D, Quastel DM (1965) A quantitative study of end-plate potentials in isolated human muscle. J Physiol 178:505-529.

20. Fasshauer D, Sutton RB, Brunger AT, Jahn R (1998) Conserved structural features of the synaptic fusion complex: SNARE proteins reclassified as Q- and R-SNAREs. Proc Natl Acad Sci U S A 95:15781-15786.

21. Fernandez-Chacon R, Sudhof TC (1999) Genetics of synaptic vesicle function: toward the complete functional anatomy of an organelle. Annu Rev Physiol 61:753-776.

22. Fernandez-Chacon R, Wolfel M, Nishimune H, Tabares L, Schmitz F, Castellano-Munoz M, Rosenmund C, Montesinos ML, Sanes JR, Schneggenburger R, Sudhof TC (2004) The synaptic vesicle protein CSP alpha prevents presynaptic degeneration. Neuron 42:237-251.

23. Fonte V, Kapulkin V, Taft A, Fluet A, Friedman D, Link CD (2002) Interaction of intracellular beta amyloid peptide with chaperone proteins. Proc Natl Acad Sci U S A 99:9439-9444.

24. Fulop T, Radabaugh S, Smith C (2005) Activity-dependent differential transmitter release in mouse adrenal chromaffin cells. J Neurosci 25:7324-7332.

25. Gandhi SP, Stevens CF (2003) Three modes of synaptic vesicular recycling revealed by single-vesicle imaging. Nature 423:607-613.

26. Geppert M, Goda Y, Hammer RE, Li C, Rosahl TW, Stevens CF, Sudhof TC (1994) Synaptotagmin I: a major Ca2+ sensor for transmitter release at a central synapse. Cell 79:717-727.

27. Gerona RR, Larsen EC, Kowalchyk JA, Martin TF (2000) The C terminus of SNAP25 is essential for Ca(2+)-dependent binding of synaptotagmin to SNARE complexes. J Biol Chem 275:6328-6336.

28. Gillis KD, Mossner R, Neher E (1996) Protein kinase C enhances exocytosis from chromaffin cells by increasing the size of the readily releasable pool of secretory granules. Neuron 16:1209-1220.

29. Hamill OP, Marty A, Neher E, Sakmann B, Sigworth FJ (1981) Improved patch-clamp techniques for high-resolution current recording from cells and cell-free membrane patches. Pflugers Arch 391:85-100.

30. Hodgkin AL, Huxley AF (1952) A quantitative description of membrane current and its application to conduction and excitation in nerve. J Physiol 117:500-544.

31. Huang C, Mason JT (1978) Geometric packing constraints in egg phosphatidylcholine vesicles. Proc Natl Acad Sci U S A 75:308-310.

32. Jagadish MN, Fernandez CS, Hewish DR, Macaulay SL, Gough KH, Grusovin J, Verkuylen A, Cosgrove L, Alafaci A, Frenkel MJ, Ward CW (1996) Insulin-

responsive tissues contain the core complex protein SNAP-25 (synaptosomal-associated protein 25) A and B isoforms in addition to syntaxin 4 and synaptobrevins 1 and 2. Biochem J 317 (Pt 3):945-954.

33. Jahn R, Sudhof TC (1994) Synaptic vesicles and exocytosis. Annu Rev Neurosci 17:219-246.

34. Jahn R, Sudhof TC (1999) Membrane fusion and exocytosis. Annu Rev Biochem 68:863-911.

35. Johannes L, Lledo PM, Chameau P, Vincent JD, Henry JP, Darchen F (1998) Regulation of the Ca2+ sensitivity of exocytosis by Rab3a. J Neurochem 71:1127-1133.

36. Kashani AH, Chen BM, Grinnell AD (2001) Hypertonic enhancement of transmitter release from frog motor nerve terminals: Ca2+ independence and role of integrins. J Physiol 530:243-252.

37. Korteweg N, Maia AS, Thompson B, Roubos EW, Burbach JP, Verhage M (2005) The role of Munc18-1 in docking and exocytosis of peptide hormone vesicles in the anterior pituitary. Biol Cell 97:445-455.

38. Lin RC, Scheller RH (2000) Mechanisms of synaptic vesicle exocytosis. Annu Rev Cell Dev Biol 16:19-49.

39. Liou ST, Wang C (2005) Small glutamine-rich tetratricopeptide repeat-containing protein is composed of three structural units with distinct functions. Arch Biochem Biophys 435:253-263.

40. Matos MF, Mukherjee K, Chen X, Rizo J, Sudhof TC (2003) Evidence for SNARE zippering during Ca2+-triggered exocytosis in PC12 cells. Neuropharmacology 45:777-786.

41. Nagy A, Baker RR, Morris SJ, Whittaker VP (1976) The preparation and characterization of synaptic vesicles of high purity. Brain Res 109:285-309.

42. Nagy G, Reim K, Matti U, Brose N, Binz T, Rettig J, Neher E, Sorensen JB (2004) Regulation of releasable vesicle pool sizes by protein kinase A-dependent phosphorylation of SNAP-25. Neuron 41:417-429.

43. Neher E, Sakmann B (1976) Single-channel currents recorded from membrane of denervated frog muscle fibres. Nature 260:799-802.

44. Oheim M, Loerke D, Stuhmer W, Chow RH (1998) The last few milliseconds in the life of a secretory granule. Docking, dynamics and fusion visualized by total internal reflection fluorescence microscopy (TIRFM). Eur Biophys J 27:83-98.

45. Olkkonen VM, Liljestrom P, Garoff H, Simons K, Dotti CG (1993) Expression of heterologous proteins in cultured rat hippocampal neurons using the Semliki Forest virus vector. J Neurosci Res 35:445-451.

46. Oyler GA, Higgins GA, Hart RA, Battenberg E, Billingsley M, Bloom FE, Wilson MC (1989) The identification of a novel synaptosomal-associated protein, SNAP-25, differentially expressed by neuronal subpopulations. J Cell Biol 109:3039-3052.

47. Pawlak V, Schupp BJ, Single FN, Seeburg PH, Kohr G (2005) Impaired synaptic scaling in mouse hippocampal neurones expressing NMDA receptors with reduced calcium permeability. J Physiol 562:771-783.

48. Perez-Otano I, Ehlers MD (2005) Homeostatic plasticity and NMDA receptor trafficking. Trends Neurosci 28:229-238.

49. Poulain B, De Paiva A, Deloye F, Doussau F, Tauc L, Weller U, Dolly JO (1996) Differences in the multiple step process of inhibition of neurotransmitter release induced by tetanus toxin and botulinum neurotoxins type A and B at Aplysia synapses. Neuroscience 70:567-576.

50. Prasher DC, Eckenrode VK, Ward WW, Prendergast FG, Cormier MJ (1992) Primary structure of the Aequorea victoria green-fluorescent protein. Gene 111:229-233.

51. Quastel DM, Hackett JT, Cooke JD (1971) Calcium: is it required for transmitter secretion? Science 172:1034-1036.

52. Rettig J, Neher E (2002) Emerging roles of presynaptic proteins in Ca++-triggered exocytosis. Science 298:781-785.

53. Rettig J, Sheng ZH, Kim DK, Hodson CD, Snutch TP, Catterall WA (1996) Isoform-specific interaction of the alpha1A subunits of brain Ca2+ channels with the presynaptic proteins syntaxin and SNAP-25. Proc Natl Acad Sci U S A 93:7363-7368.

54. Richards DA, Bai J, Chapman ER (2005) Two modes of exocytosis at hippocampal synapses revealed by rate of FM1-43 efflux from individual vesicles. J Cell Biol 168:929-939.

55. Richmond JE, Davis WS, Jorgensen EM (1999) UNC-13 is required for synaptic vesicle fusion in C. elegans. Nat Neurosci 2:959-964.

56. Rizo J, Sudhof TC (2002) Snares and Munc18 in synaptic vesicle fusion. Nat Rev Neurosci 3:641-653.

57. Rizzoli SO, Betz WJ (2005) Synaptic vesicle pools. Nat Rev Neurosci 6:57-69.

58. Rosenmund C, Stevens CF (1996) Definition of the readily releasable pool of vesicles at hippocampal synapses. Neuron 16:1197-1207.

59. Roth D, Burgoyne RD (1994) SNAP-25 is present in a SNARE complex in adrenal chromaffin cells. FEBS Lett 351:207-210.

60. Sakaba T, Stein A, Jahn R, Neher E (2005) Distinct kinetic changes in neurotransmitter release after SNARE protein cleavage. Science 309:491-494.

61. Schantl JA, Roza M, De Jong AP, Strous GJ (2003) Small glutamine-rich tetratricopeptide repeat-containing protein (SGT) interacts with the ubiquitin-dependent endocytosis (UbE) motif of the growth hormone receptor. Biochem J 373:855-863.

62. Schluter OM, Khvotchev M, Jahn R, Sudhof TC (2002) Localization versus function of Rab3 proteins. Evidence for a common regulatory role in controlling fusion. J Biol Chem 277:40919-40929.

63. Schluter OM, Basu J, Sudhof TC, Rosenmund C (2006) Rab3 superprimes synaptic vesicles for release: implications for short-term synaptic plasticity. J Neurosci 26:1239-1246.

64. Schluter OM, Schmitz F, Jahn R, Rosenmund C, Sudhof TC (2004) A complete genetic analysis of neuronal Rab3 function. J Neurosci 24:6629-6637.

65. Schneggenburger R, Meyer AC, Neher E (1999) Released fraction and total size of a pool of immediately available transmitter quanta at a calyx synapse. Neuron 23:399-409.

66. Shimoni Y, Alnaes E, Rahamimoff R (1977) Is hyperosmotic neurosecretion from motor nerve endings a calcium-dependent process? Nature 267:170-172.

67. Smith C, Moser T, Xu T, Neher E (1998) Cytosolic Ca2+ acts by two separate pathways to modulate the supply of release-competent vesicles in chromaffin cells. Neuron 20:1243-1253.

68. Sorensen JB, Wiederhold K, Muller EM, Milosevic I, Nagy G, de Groot BL, Grubmuller H, Fasshauer D (2006) Sequential N- to C-terminal SNARE complex assembly drives priming and fusion of secretory vesicles. Embo J 25:955-966.

69. Stevens CF, Tsujimoto T (1995) Estimates for the pool size of releasable quanta at a single central synapse and for the time required to refill the pool. Proc Natl Acad Sci U S A 92:846-849.

70. Stevens DR, Wu ZX, Matti U, Junge HJ, Schirra C, Becherer U, Wojcik SM, Brose N, Rettig J (2005) Identification of the minimal protein domain required for priming activity of Munc13-1. Curr Biol 15:2243-2248.

71. Sudhof TC (1995) The synaptic vesicle cycle: a cascade of protein-protein interactions. Nature 375:645-653.

72. Sugimori M, Lang EJ, Silver RB, Llinas R (1994) High-resolution measurement of the time course of calcium-concentration microdomains at squid presynaptic terminals. Biol Bull 187:300-303.

73. Sutton RB, Fasshauer D, Jahn R, Brunger AT (1998) Crystal structure of a SNARE complex involved in synaptic exocytosis at 2.4 A resolution. Nature 395:347-353.

74. Takeuchi A (1958) The long-lasting depression in neuromuscular transmission of frog. Jpn J Physiol 8:102-113.

75. Taraska JW, Perrais D, Ohara-Imaizumi M, Nagamatsu S, Almers W (2003) Secretory granules are recaptured largely intact after stimulated exocytosis in cultured endocrine cells. Proc Natl Acad Sci U S A 100:2070-2075.

76. Taschenberger H, Scheuss V, Neher E (2005) Release kinetics, quantal parameters and their modulation during short-term depression at a developing synapse in the rat CNS. J Physiol 568:513-537.

77. Thies RE (1965) Neuromuscular Depression and the Apparent Depletion of Transmitter in Mammalian Muscle. J Neurophysiol 28:428-442.

78. Tobaben S, Varoqueaux F, Brose N, Stahl B, Meyer G (2003) A brain-specific isoform of small glutamine-rich tetratricopeptide repeat-containing protein binds to Hsc70 and the cysteine string protein. J Biol Chem 278:38376-38383.

79. Tobaben S, Thakur P, Fernandez-Chacon R, Sudhof TC, Rettig J, Stahl B (2001) A trimeric protein complex functions as a synaptic chaperone machine. Neuron 31:987-999.

80. Trudeau LE, Fang Y, Haydon PG (1998) Modulation of an early step in the secretory machinery in hippocampal nerve terminals. Proc Natl Acad Sci U S A 95:7163-7168.

81. Turrigiano GG, Nelson SB (2004) Homeostatic plasticity in the developing nervous system. Nat Rev Neurosci 5:97-107.

82. Voets T, Toonen RF, Brian EC, de Wit H, Moser T, Rettig J, Sudhof TC, Neher E, Verhage M (2001) Munc18-1 promotes large dense-core vesicle docking. Neuron 31:581-591.

83. Walch-Solimena C, Blasi J, Edelmann L, Chapman ER, von Mollard GF, Jahn R (1995) The t-SNAREs syntaxin 1 and SNAP-25 are present on organelles that participate in synaptic vesicle recycling. J Cell Biol 128:637-645.

84. Wang H, Shen H, Wang Y, Li Z, Yin H, Zong H, Jiang J, Gu J (2005) Overexpression of small glutamine-rich TPR-containing protein promotes apoptosis in 7721 cells. FEBS Lett 579:1279-1284.

85. Wang Y, Sudhof TC (2003) Genomic definition of RIM proteins: evolutionary amplification of a family of synaptic regulatory proteins(small star, filled). Genomics 81:126-137.

86. Wang Y, Dulubova I, Rizo J, Sudhof TC (2001) Functional analysis of conserved structural elements in yeast syntaxin Vam3p. J Biol Chem 276:28598-28605.

87. Weclewicz K, Svensson L, Kristensson K (1998) Targeting of endoplasmic reticulum-associated proteins to axons and dendrites in rotavirus-infected neurons. Brain Res Bull 46:353-360.

88. Wei S, Xu T, Ashery U, Kollewe A, Matti U, Antonin W, Rettig J, Neher E (2000) Exocytotic mechanism studied by truncated and zero layer mutants of the C-terminus of SNAP-25. Embo J 19:1279-1289.

89. Weimbs T, Low SH, Chapin SJ, Mostov KE, Bucher P, Hofmann K (1997) A conserved domain is present in different families of vesicular fusion proteins: a new superfamily. Proc Natl Acad Sci U S A 94:3046-3051.

90. Weimer RM, Richmond JE (2005) Synaptic vesicle docking: a putative role for the Munc18/Sec1 protein family. Curr Top Dev Biol 65:83-113.

91. Winnefeld M, Rommelaere J, Cziepluch C (2004) The human small glutamine-rich TPR-containing protein is required for progress through cell division. Exp Cell Res 293:43-57.

92. Winnefeld M, Grewenig A, Schnolzer M, Spring H, Knoch TA, Gan EC, Rommelaere J, Cziepluch C (2006) Human SGT interacts with Bag-6/Bat-3/Scythe and cells with reduced levels of either protein display persistence of few misaligned chromosomes and mitotic arrest. Exp Cell Res 312:2500-2514.

93. Wu LG, Borst JG (1999) The reduced release probability of releasable vesicles during recovery from short-term synaptic depression. Neuron 23:821-832.

94. Xu T, Binz T, Niemann H, Neher E (1998) Multiple kinetic components of exocytosis distinguished by neurotoxin sensitivity. Nat Neurosci 1:192-200.

95. Xu T, Ashery U, Burgoyne RD, Neher E (1999a) Early requirement for alpha-SNAP and NSF in the secretory cascade in chromaffin cells. Embo J 18:3293-3304.

96. Xu T, Rammner B, Margittai M, Artalejo AR, Neher E, Jahn R (1999b) Inhibition of SNARE complex assembly differentially affects kinetic components of exocytosis. Cell 99:713-722.

97. Yin H, Wang H, Zong H, Chen X, Wang Y, Yun X, Wu Y, Wang J, Gu J (2006) SGT, a Hsp90beta binding partner, is accumulated in the nucleus during cell apoptosis. Biochem Biophys Res Commun 343:1153-1158.

98. Zenchenko TA, Morozov VN (1995) Mechanical deformation enhances catalytic activity of crystalline carboxypeptidase A. Protein Sci 4:251-257.

99. Zenisek D, Steyer JA, Almers W (2000) Transport, capture and exocytosis of single synaptic vesicles at active zones. Nature 406:849-854.

100. Zucker RS (1989) Short-term synaptic plasticity. Annu Rev Neurosci 12:13-31.

101. Zucker RS, Regehr WG (2002) Short-term synaptic plasticity. Annu Rev Physiol 64:355-405.

7. Publications /acknowledgment

Publications are in progress:

……………………………………………………………

……………………………………………………………

……………………………………………………………

8. Curriculum vitae

PERSÖNLICHE DATEN

Name:	Stefan Nikolaus Linsler
	geboren am 24.11.1980 in Saarlouis
Anschrift:	Ringstraße 67, 66424 Homburg, Deutschland
Email:	stli5001@stud.uni-saarland.de
Familienstand:	ledig
Staatsangehörigkeit:	deutsch

AUSBILDUNG

1987 – 1991	Besuch der Grundschule Griesborn
1991 – 2000	Besuch des Saarlouiser Gymnasiums am Stadtgarten mit dem Abitur als Abschluss
Juli – Oktober 2000	Rettungssanitäterausbildung im Rahmen des Zivildienstes
Juni 2001	Sprachkurs in Medical English in Oxford
Seit Oktober 2001	Medizinstudium an der medizinischen Fakultät der Universität des Saarlandes in Homburg/Saar
Seit April 2003	Stipendiat im Cusanuswerk (deutsches Hochbegabten-förderungswerk)
August 2003	Absolvierung des Physikums
Seit April 2004	Promotion am physiologischen Institut der medizinischen Fakultät in der Abteilung von Prof. Dr. J. Rettig
	Erlernte Fremdsprachen: Englisch, Französisch, Latein

BISHERIGE TÄTIGKEITEN

Juli 2000–Juni 2001	Zivildienst als Rettungssanitäter in der Rettungswache des Deutschen Roten Kreuzes in Dillingen/ Saar
August 2000	Krankenpflegepraktikum auf der Intensivstation des Städtischen Krankenhauses in Dillingen/Saar

Juli 2001	Krankenpflegepraktikum in der Inneren Abteilung des DRK Krankenhauses in Saarlouis
Sommersemester 2003	Tutor im biochemischen Praktikum für Mediziner
Wintersemester 03/04	Moniteur im Anatomiekurs für Mediziner
März 2004	Famulatur in der Angiologie und Stroke Unit des DRK Krankenhauses in Saarlouis
Sommersemester 2004	Tutor im physiologischen Praktikum für Mediziner und Pharmazeuten
August 2004	Summerschool im International Hospital in Sharm El Sheikh/Ägypten zum Thema „Tauchmedizin" im hyperbaren Druckkammerzentrum des Krankenhauses
September 2004	Famulatur in einer pädiatrischen Praxis in Saarlouis
Wintersemester 04/05	Moniteur im Anatomiekurs für Mediziner
März/April 2005	Famulatur als Unterassistent in der Orthopädie/Traumatologie des Spitals Rorschach
September 2005	Famulatur in Wuhan/ VR China in der Abteilung für TCM und Neurochirurgie
Wintersemester 05/06	Moniteur im Anatomiekurs für Mediziner
März 2006	Famulatur in der Abteilung für Anästhesiologie der Universitätsklinik Homburg
Sommersemester 2006	Tutor im physiologischen Praktikum für Mediziner und Pharmazeuten
Seit August 2006	PJ: erstes PJ-Tertial in der neurochirurgischen Klinik der Universitätskliniken Homburg; zweites Tertial in der chirurgischen Abteilung des Kantonspitals Bruderholz/ Schweiz; drittes Tertial in der Inneren Medizin der University of Toronto/Kanada

HOBBIES

Ich bin Mitglied in der DLRG (Deutsche Lebensrettungsgesellschaft) und bin dort als Rettungsschwimmer, Rettungstaucher, Sanitätsausbilder sowie als Referent Medizin des Landesverbandes Saar tätig.